Acoustic and hydrodynamic power of wave scattering by an infinite cascade of plates in mean flow

Georg Maierhofer[a,*], N. Peake[b]

[a] *Laboratoire Jacques-Louis Lions, Sorbonne University, France*
[b] *Department of Applied Mathematics and Theoretical Physics, University of Cambridge, UK*

Abstract

We study the balance of outgoing and incoming power for acoustic wave scattering by a cascade of flat blades in uniform subsonic mean flow. In nonzero mean flow the Kutta condition at the trailing edge of the cascade plates leads to the production of vorticity in the form of unsteady vortex sheets attached at the trailing edges, which results in a hydrodynamic power flux and the exchange of energy between the unsteady vorticity and the acoustic field. Although the scattering problem itself has been subject to much previous research, a comprehensive study of the composition of the outgoing energy flux for cascade scattering has received little previous attention. As an application of our detailed study we show how the time-averaged energy balance can be used to explain certain symmetries of the field in the angle of incidence with respect to the cascade face when there is no mean flow and the effect of zero acoustic reflection at certain angles of incidence with mean flow. We also show that, depending on the angle of incidence of the acoustic wave and the velocity of the mean flow, the vortex sheets can either absorb or generate acoustic energy. This can, for certain parameter values, result in a net increase in outgoing sound power over the incident sound power, as we demonstrate on a number of numerical examples that are computed using the semi-analytical solution described in recent work by Maierhofer & Peake [1].

Keywords: energy balance, acoustic scattering, sound power, acoustic energy dissipation
2010 MSC: 76Q05

1. Introduction

We consider an infinite cascade of blades with zero thickness and camber placed in subsonic mean flow aligned with the blade chord, and are interested

*Corresponding author
Email address: georg.maierhofer@sorbonne-universite.fr (Georg Maierhofer)

in understanding the balance of acoustic and hydrodynamic power that is scattered when the geometry is subjected to an incident acoustic wave from either upstream or downstream. This particular geometry has been of scientific interest for several decades due to its use as a basic model for blade rows in turbomachinery. The solution of the scattering problem with and without subsonic mean flow is widely studied, with a number of techniques readily available in the literature.

One way to approach this scattering problem is via a solution of the Ffowcs Williams & Hawkings equation [2] providing a model for the noise generation of the fluid structure interaction with the cascade blades. However, it turns out that linearised and inviscid approximations also provide a simple and suitable way of solving the problem, and that in this setting the boundary effects on the flat plates can be accounted for including by imposing a Kutta condition at the trailing edges of the cascade [3]. These inviscid equations can be solved using the Wiener–Hopf technique, an approach that was first taken in this geometry by Koch [4] who provided explicit expressions for the far-field unsteady potential based on the solution of an infinite algebraic system. Peake [5, 6] derived expressions for the detailed unsteady lift distribution on the blades, and increased the efficiency of these methods using asymptotic kernel factorisations. Glegg [7] provided a study of sound power, by considering only the acoustic power that is scattered from the cascade. We will see in this paper that our work extends on this by accounting for the hydrodynamic power in the wake and an acoustic energy exchange term associated with the unsteady vortex sheet attached to the trailing edge, which together with the acoustic power allow a full balance of incoming and outgoing power. Finally, we mention recent work by Maierhofer & Peake [1] which removes a crucial assumption on the spacing of these cascades, shared by the aforementioned methods, to allow for arbitrary spacing of consecutive plates and in this current work we shall rely on the numerical method provided by [1]. In addition to the above-mentioned work there is a range of research that extends this Wiener–Hopf analysis to allow for realistic features such as for instance blade mean loading and realistic blade geometry (Peake & Kerschen [8, 9], Evers & Peake [10] and Baddoo & Ayton [11]) and complex boundary conditions such as porosity (Baddoo & Ayton [12]).

Despite the large amount of attention given to the solution of the scattering problem and the computation of modal amplitudes of the scattered field, the balance of incoming and outgoing energy flux in the cascade of blades has remained largely unstudied. In the presence of nonzero mean flow, the vorticity shed from the trailing edges can interact with the acoustic field and provide a mechanism for energy exchange between the mean flow and the acoustic field, which has interesting ramifications on the conservation of acoustic energy. The consequences of this energy exchange were subject of a large amount of research in the 1960's and early 1970's, for instance by Cantrell & Hart [13], Möhring [14, 15] and Morfey [16], and it was realised only towards the late 1970's and 1980's through the exact relations given by Goldstein [17] and Myers [18, 19] that acoustic energy in the presence of vorticity is no longer conserved.

The possibility of the generation of sound through vorticity was, of course, well-known since the pioneering work by Lighthill [20], and appears for instance in the Ffowcs Williams acoustic analogy of turbulence passing a trailing edge [21] and in Crighton's model problem of a vortex passing an edge [22]. However, the possibility of attenuation of sound by vorticity was confirmed experimentally only several years later in the work by Bechert et al. [23], who found conclusive evidence of sound attenuation in a pure tone exiting a cylindrical nozzle with mean flow.

The sound attenuation observed in [23] was explained analytically by Howe [24, 25] (with further detail provided in his later work [26, 27]), as the acoustic energy loss arising from vortex shedding at the sharp trailing edges of the nozzle. However, in his analysis Howe did not distinguish between the acoustic energy converted into hydrodynamic (pressureless) potential perturbations and energy flux into the vortex sheet. The complete energy balance was first provided in the context of annular ducts by Rienstra [28] who essentially found all the same terms that appear in the energy balance for the cascade of blades which we study in the present work. A further interesting observation was made by Rienstra [29] who, in explicitly calculating the acoustic energy flux into the wake for single sharp trailing edges in two dimensions, found that energy can be exchanged in both directions between acoustic and vortical components of the field. In the present work we confirm that also for blade rows this effect can lead both to significant attenuation as well as to the production of sound.

The sound attenuation through the production of vorticity is highly relevant to fluid mechanical engineering systems, including to turbomachinery, since the attenuation of sound is a very favourable by-product of the geometry and needs to be taken into account for noise prediction schemes. The main novelty of the present work is that we provide a detailed study of the energy balance in the case of an infinite cascade of plates. In particular we account for all contributions to the outgoing power – acoustic power, hydrodynamic power and energy flux into the wake. Whilst accounting for all relevant contributions we also provide an overview of several physical interpretations of these terms offered by the literature, including the exchange of acoustic energy with the vortex sheets which can be thought of as the work done by a lift force, as has been observed by Howe [30] for general edges, and by Guo [31] for a single trailing edge in supersonic flow. We also place this analysis in the context of incompressible literature where an analogous energy exchange term was found by Arzoumanian [32] to be of the same form as the interface flux that appears when an elastic sheet is placed in an incompressible fluid (as studied by Crighton & Oswell [33]). Our expressions allow us to conduct numerical experiments from which we can draw a number of interesting conclusions. Specifically, the energy exchange term and the hydrodynamic power account in many parameter settings for a significant portion of the outgoing energy. We confirm that in the case of a cascade the acoustic energy flux into the wake can be negative, which means the cascade can harvest energy from the flow. This leads to additional energy in the scattered acoustic field and in some cases can result in an amplification of the acoustic power, and over-reflection, whereby the scattered acoustic field

has a larger amplitude than the incoming acoustic field.

In addition to the numerical experiments, our expressions for the power balance can be used to infer properties of the far-field, such as symmetries with respect to certain angles of incidence and perfect transmission at specific angles of attack. The latter is related to recent work by Porter [34], who studied perfectly transmitting blade rows in zero mean flow in the context of metamaterials, and we are able to show that some of his conclusions extend to the case when nonzero mean flow is present.

The present manuscript is structured as follows: §2 provides a brief recap of the mathematical formulation of the scattering problem for a cascade of blades, as is found in the literature. We outline the form of the total field away from the cascade (consisting of radiating acoustic and hydrodynamic modes) and quote the explicit expression for these modes. In §3 we derive the energy balance for this system based on the usual form of conservation of acoustic energy given by Goldstein [17], and we include a discussion outlining the interpretation of the energy exchange term in the context of the relevant literature. This section includes an explicit form of the time-averaged energy balance in terms of the modal amplitudes of the total field. These expressions are used in §4 to study symmetries in the field and to give numerical examples to understand the form of each contribution to the energy balance. Conclusions and a brief outlook for future research are provided in §5.

2. Problem statement

For completeness we briefly recap the mathematical formulation of the system and corresponding boundary and edge conditions. In our formulation we rescale physical quantities as follows: lengths are scaled by l the blade chord, times by l/U_∞, density perturbations by the undisturbed fluid density ρ_0, pressure fluctuations by $\rho_0 U_\infty^2$, and we let $M := U/c_0$ be the subsonic Mach number of the flow. Finally, the normalised blade stagger d, and interblade spacing s are defined as in Fig. 1, resulting in the stagger angle $\alpha_0 = \arctan(s/d)$.

Our two-dimensional geometry consists of an infinitely extending cascade of plates located at $\{(x, ns) \,\big|\, nd < x < nd + 1\}$, $n \in \mathbb{Z}$. We note that the inclusion of a third dimension, with a given spanwise wavenumber, does not involve any conceptual difficulties (indeed has been implemented in the literature [7, 1]) but it would complicate some of the algebraic expressions in this work. We assume the incidence of harmonic acoustic waves on the cascade with reduced frequency Ω, amplitude I, and normal to the wavefronts that is inclined at an angle φ as shown in Fig. 1.

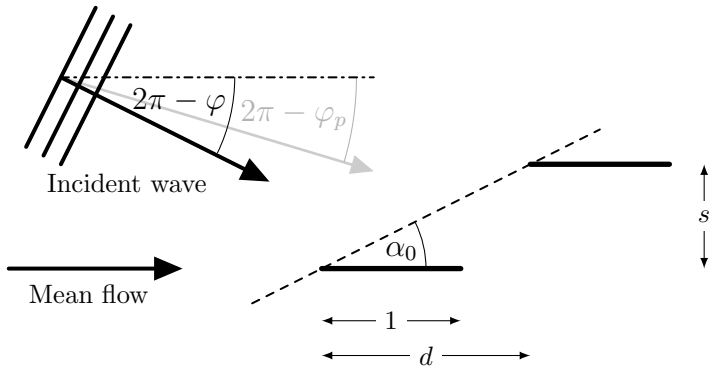

Figure 1: Sketch of cascade of blades with incident upstream acoustic wave.

As a result, all quantities describing the perturbed flow are time-harmonic, and indeed can be expressed in terms of a velocity potential $\exp(\mathrm{i}\Omega t)\phi(x, y)$, which is the sum of an incoming wave and a scattered potential:

$$\phi(x, y) = I\mathrm{e}^{-\mathrm{i}k_x x - \mathrm{i}k_y y} + \phi_s(x, y),$$

where

$$k_x = \Omega M \frac{\cos\varphi}{1 + M\cos\varphi}, \quad k_y = \Omega M \frac{\sin\varphi}{1 + M\cos\varphi}. \tag{1}$$

Due to the presence of nonzero mean flow the energy of the waves propagates at an angle φ_p (also highlighted in Fig. 1) which is, in general, different from φ. The angle of propagation φ_p is a fundamental physical property of the field and there is a simple one-to-one correspondence between φ_p and φ (see for instance [29, §4]) given by

$$\cos\varphi_p = \frac{\cos\varphi + M}{(1 + 2M\cos\varphi + M^2)^{\frac{1}{2}}}, \quad \sin\varphi_p = \frac{\sin\varphi}{(1 + 2M\cos\varphi + M^2)^{\frac{1}{2}}} \tag{2}$$

This correspondence is found from explicit computation of the time-averaged acoustic energy flux of the incident wave as is shown in Eqs. (14)-(15) below. Hence we see that all of the derivations shown in the present work which are given in terms of φ could also equivalently be expressed in terms of φ_p.

The total velocity potential must then satisfy the two-dimensional convected wave equation:

$$\frac{\mathrm{D}^2\phi}{\mathrm{D}t^2} - M^{-2}\Delta\phi = 0, \tag{3}$$

where the non-dimensional material derivative for time-harmonic quantities is given by $\mathrm{D}/\mathrm{D}t = \mathrm{i}\Omega + \partial_x$. In addition to the equation of motion the following boundary conditions are assumed in order to find a physically valid solution to the problem:

(i) The cascade blades are acoustically hard, such that

$$\frac{\partial \phi}{\partial y} = 0 \text{ on } \{0 \leq x - nd \leq 1, y = ns\}.$$

(ii) The unsteady pressure, which is given to leading order by the momentum equation as

$$p = -\frac{\mathrm{D}\phi}{\mathrm{D}t},$$

is continuous away from the blades.

(iii) The scattered field must satisfy a radiation condition, which effectively stipulates that waves must be outgoing upstream and downstream of the cascade. An effective way of distinguishing between outgoing and incoming waves is to introduce a small fictitious damping, equivalent to a small negative imaginary part of the frequency, $\mathrm{Im}\,\Omega < 0$, and to require that outgoing waves are bounded at $x = \pm\infty$ respectively. More details about this assumption can be found e.g. in [6], and are not repeated in this work.

(iv) A shift in $(x, y) \mapsto (x + d, y + s)$ results in a shift in phase of the incident acoustic wave. We require the scattered potential to exhibit a similar property, namely for all $(x, y) \in \mathbb{R}^2, n \in \mathbb{Z}$:

$$\phi(x, y) = \mathrm{e}^{-\mathrm{i}n\sigma}\phi(x + nd, y + ns),$$

where, according to Eq. (1)

$$\sigma = -\frac{\Omega M}{1 + M\cos\varphi}(d\cos\varphi + s\sin\varphi). \tag{4}$$

This is essentially a Bloch condition as we move from one cell $\{(x, y) \,\big|\, -\infty < x < \infty, ns \leq y \leq (n+1)s\}$ in the cascade to the next, and σ is often referred to as the inter-blade phase angle. Thus we may focus our attention to the first cell and recover the solution elsewhere by a simple shift of phase.

(v) The total velocity normal to the blades $\frac{\partial \phi}{\partial y}$ must be continuous everywhere (which follows from the continuity of pressure and the consideration of infinitely thin blades).

(vi) The scattered field satisfies the Kutta condition at the trailing edge (see for instance [5, 3]), i.e. the pressure jump $[p](x, y) = p(x, y^+) - p(x, y^-)$ is non-singular at the points $(x, y) = (1 + nd, ns)$, and the usual inverse square-root singularity at the leading edge, i.e. ϕ has an inverse square-root singularity at the points $(x, y) = (nd, ns)$.

As mentioned before, several techniques are available in the literature which can solve this type of problem.

2.1. Dispersion relation for free space solutions

In this work we are specifically interested in the energy transported to the far-field, thus let us begin by considering the kind of waves that exist in the parts of the geometry away from the cascade structure. Fourier transforming Eq. (3) in the x coordinate yields for time-harmonic waves:

$$\frac{\partial^2}{\partial y^2}\Phi = \gamma(\alpha)^2\Phi,$$

where $\gamma(\alpha)^2 = \alpha^2(1-M^2) + 2\alpha\Omega M^2 - \Omega^2 M^2$ and

$$\Phi(\alpha; y) = \int_{-\infty}^{\infty} \mathrm{e}^{\mathrm{i}\,\alpha x}\phi(x,y)\,\mathrm{d}x.$$

Thus solutions which satisfy (iv) & (v) must be of the following form when $0 < y < s$:

$$\Phi(\alpha; y) = A(\alpha)\underbrace{\left(\cosh\gamma y - \mathrm{e}^{-\mathrm{i}\,\sigma - \mathrm{i}\,d\alpha}\cosh\gamma(y-s)\right)}_{=:f(\alpha,y)}. \tag{5}$$

To impose continuity of pressure away from the blades we consider the (spatial component of the) pressure difference across $y = 0$, which, using (iv) to relate the value of p in the cascade cell $-s < y < 0$ with the corresponding value in $0 < y < s$, is given by

$$\begin{aligned}
[P](\alpha) &= \int_{-\infty}^{\infty} \mathrm{e}^{\mathrm{i}\,\alpha x}\left(p(x,0^+) - p(x,0^-)\right)\mathrm{d}x \\
&= \int_{-\infty}^{\infty} \mathrm{e}^{\mathrm{i}\,\alpha x}\left(p(x,0^+) - \mathrm{e}^{-\mathrm{i}\,\sigma}p(x+d,s^-)\right)\mathrm{d}x \\
&= -\int_{-\infty}^{\infty} \mathrm{e}^{\mathrm{i}\,\alpha x}\frac{\mathrm{D}}{\mathrm{D}t}\left(\phi(x,0^+) - \mathrm{e}^{-\mathrm{i}\,\sigma}\phi(x+d,s^-)\right)\mathrm{d}x \\
&= -(\mathrm{i}\,\Omega - \mathrm{i}\,\alpha)\left(\Phi(\alpha,0^+) - \mathrm{e}^{-\mathrm{i}\,\sigma - \mathrm{i}\,d\alpha}\Phi(\alpha,s^-)\right) \\
&= \underbrace{-2\mathrm{e}^{-\mathrm{i}\,\sigma - \mathrm{i}\,d\alpha}(\mathrm{i}\,\omega - \mathrm{i}\,\alpha)\left(\cos(\sigma + d\alpha) - \cosh\gamma s\right)}_{=:D(\alpha)}A(\alpha)
\end{aligned}$$

Thus, imposing continuity of pressure for $x \notin [0,1]$, i.e. condition (ii), and inverting the field, we find the expression

$$\begin{aligned}
\phi(x,y) &= \frac{1}{2\pi}\int_{-\infty}^{\infty} \mathrm{e}^{-\mathrm{i}\,x\alpha}\frac{f(\alpha,y)}{D(\alpha)}[P](\alpha)\,\mathrm{d}\alpha \\
&= \frac{1}{2\pi}\int_{-\infty}^{\infty} \mathrm{e}^{-\mathrm{i}\,x\alpha}\frac{f(\alpha,y)}{D(\alpha)}\int_0^1 [p](\tilde{x})\,\mathrm{d}\tilde{x}\,\mathrm{d}\alpha.
\end{aligned} \tag{6}$$

The zeros of $D(\alpha)$ therefore give rise to wave-like modes away from the cascade structure (i.e. modes which are x-harmonic if $sx < dy$ or $s(x-1) > dy$).

Therefore the dispersion relation for modal solutions in free space away from the cascade structure is given by

$$D(\alpha) = 0. \tag{7}$$

The solutions to Eq. (7) are the acoustic modes, $\alpha = \sigma_m^{\pm}(\Omega),\ m \in \mathbb{Z}$, with the superscript $\pm$ denoting upstream and downstream travelling modes respectively, and the hydrodynamic mode, $\alpha = \Omega$, which is convected with the dimensional mean-flow speed. The analytical expressions for the acoustic modes are, for $-r \leq m \leq q$:

$$\begin{aligned}\sigma_m^{\pm} = &\frac{-(s^2M^2\Omega + d\sigma + 2d\pi m)}{s^2\beta^2 + d^2} \\ &\mp \frac{\sqrt{(s^2M^2\Omega + d\sigma + 2d\pi m)^2 - (s^2\beta^2 + d^2)\left((\sigma + 2\pi m)^2 - s^2\Omega^2M^2\right)}}{s^2\beta^2 + d^2},\end{aligned} \tag{8}$$

and for $m > q, m < -r$:

$$\begin{aligned}\sigma_m^{\pm} = &\frac{-(s^2M^2\Omega + d\sigma + 2d\pi m)}{s^2\beta^2 + d^2} \\ &\pm \frac{\mathrm{i}\sqrt{-(s^2M^2\Omega + d\sigma + 2d\pi m)^2 + (s^2\beta^2 + d^2)\left((\sigma + 2\pi m)^2 - s^2\Omega^2M^2\right)}}{s^2\beta^2 + d^2},\end{aligned}$$

with $-r, q$ being the smallest and largest integer respectively such that

$$\left(s^2M^2\Omega + d\sigma + 2d\pi m\right)^2 - (s^2\beta^2 + d^2)\left((\sigma + 2\pi m)^2 - s^2\Omega^2M^2\right) \geq 0.$$

In the above we denoted $\beta^2 = 1 - M^2$. The acoustic modes $\sigma_m^{\pm}(\Omega)$ with $-r \leq m \leq q$ lie on the real line and give rise to non-vanishing wave-like solutions at $x = \pm\infty$, which we call *cut-on modes*. The remaining acoustic modes lie in the complex plane away from the real axis and contribute to evanescent effects. These modes are called *cut-off modes*. More details on the relevance of these modes in the Wiener–Hopf analysis of the scattering problem are given in [1, 5]. The dispersion curves for Eq. (7) are shown in Fig. 2.

We recall from Eq. (4) that the value of σ depends on the frequency and angle of the incident field, thus it implicitly depends on Ω. This means firstly that in the current formulation the incident acoustic wave always corresponds to $\sigma_0^{\pm}$ ($\pm$ is taken appropriately corresponding to downstream and upstream incidence respectively) and secondly that $\sigma_0^{\pm}$ are proportional to Ω, and hence give rise to the straight-line dispersion curves for $\sigma_0^{\pm}$ as observed in Fig. 2.

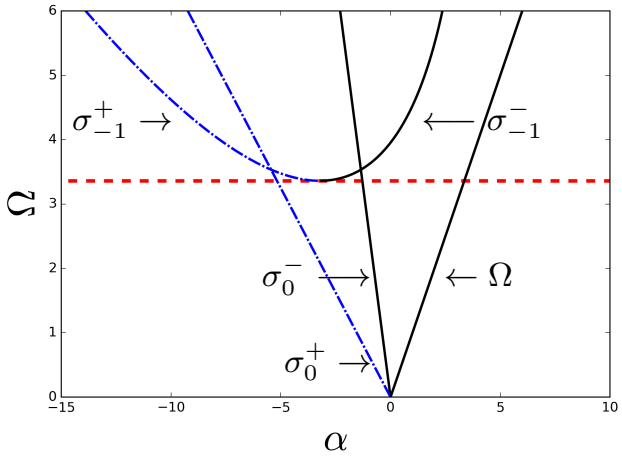

Figure 2: Dispersion curves for radiating acoustic modes away from the cascade. The dashed horizontal line marks the value of Ω for which $\sigma_{-1}^{\pm}$ become cut-on. Upstream travelling modes are marked with dash-dotted lines, downstream travelling modes correspond to the solid black lines.

2.2. Form of the incident field

For the incident acoustic waves we can verify (cf. [1, §3.1.1]) using the parametrisation Eq. (1) that

$$k_x = \begin{cases} \sigma_0^- & \text{if } s(M_x + \cos\varphi) - d\sin\varphi \geq 0, \\ \sigma_0^+ & \text{if } s(M_x + \cos\varphi) - d\sin\varphi < 0, \end{cases}$$

i.e. $k_x = \sigma_0^-$ if the incident wave is travelling downstream with respect to the cascade stagger (i.e. is incident from upstream), and $k_x = \sigma_0^+$ if the wave travels upstream (i.e. is incident from downstream). Similarly, one can check that

$$k_y = \begin{cases} \mathrm{i}\,\gamma(\sigma_0^-) & \text{if } s(M_x + \cos\varphi) - d\sin\varphi \geq 0, \\ -\mathrm{i}\,\gamma(\sigma_0^+) & \text{if } s(M_x + \cos\varphi) - d\sin\varphi < 0, \end{cases}$$

which means the incident field can be expressed as the wave mode

$$I\mathrm{e}^{-\mathrm{i}\,\sigma_0^{\mp} x \pm \gamma(\sigma_0^{\mp}) y}$$

where the signs in the above expression are to be taken appropriately depending on whether the wave is incident from upstream or from downstream.

2.3. Form of the total field away from the cascade structure

The solution of this problem is extensively studied in the literature (amongst others by [1, 4, 6, 7, 34]) and the form of time-harmonic solutions in the far-field is well-known, and is shown in Tab. 1. Note the expressions here specify ϕ in

the first cascade cell $0 \leq y < s$ and the field is determined uniquely in the remaining cells by condition (iv). Note the form of the field presented in Tab. 1 is the exact form which is valid for each coordinate (x, y) in the range indicated ($sx < dy$, and $s(x-1) > dy$ respectively). This means the evanescent modes (which, of course, do not contribute to the asymptotic far-field) are included and their contribution is important when evaluating the exchange of acoustic and vortical energy near the trailing edge as discussed in §3.

In Tab. 1 U_m, D_m are complex constants, the amplitudes of the acoustic modes travelling upstream and downstream of the cascade respectively, and the complex constant B is the amplitude of the hydrodynamic mode shed from the trailing edge of each blade. Furthermore, we have introduced the function

$$g(y) = \frac{\mathrm{e}^{\mathrm{i}\,\sigma + \mathrm{i}\,d\Omega}\cosh(\Omega y) - \cosh(\Omega(s-y))}{2(\cos(\sigma + d\Omega) - \cosh(s\Omega))}. \tag{9}$$

Table 1: Expressions for the total field with upstream and downstream incident acoustic waves.

Upstream incidence	**Downstream incidence**
Incident wavenumber: $k_x = \sigma_0^-$	Incident wavenumber: $k_x = \sigma_0^+$
Upstream ($sx < dy$)	Upstream ($sx < dy$)
$\phi(x,y) = I\mathrm{e}^{-\mathrm{i}\,\sigma_0^- x}\mathrm{e}^{\gamma(\sigma_0^-)y} + \sum_{m\in\mathbb{Z}} U_m \mathrm{e}^{-\mathrm{i}\,\sigma_m^+ x}\mathrm{e}^{-\gamma(\sigma_m^+)y}.$	$\phi(x,y) = \sum_{m\in\mathbb{Z}} U_m \mathrm{e}^{-\mathrm{i}\,\sigma_m^+ x}\mathrm{e}^{-\gamma(\sigma_m^+)y}.$
Downstream ($s(x-1) > dy$)	Downstream ($s(x-1) > dy$)
$\phi(x,y) = B\mathrm{e}^{-\mathrm{i}\,\Omega x} g(y) + \sum_{m\in\mathbb{Z}} D_m \mathrm{e}^{-\mathrm{i}\,\sigma_m^- x}\mathrm{e}^{\gamma(\sigma_m^-)y}.$	$\phi(x,y) = I\mathrm{e}^{-\mathrm{i}\,\sigma_0^+ x}\mathrm{e}^{-\gamma(\sigma_0^+)y} + B\mathrm{e}^{-\mathrm{i}\,\Omega x} g(y) + \sum_{m\in\mathbb{Z}} D_m \mathrm{e}^{-\mathrm{i}\,\sigma_m^- x}\mathrm{e}^{\gamma(\sigma_m^-)y}.$

There are several numerical and semi-analytical methods available in the literature which provide a way of computing these amplitudes for given incident fields. Amongst the numerical methods we mention early work by Whitehead [35] and Smith [36] and later work by Porter [34] all of which essentially formulate the problem in terms of an integral equation similar to Eq. (6) which is then solved by either Nyström-type methods or, in the latter work, by a Galerkin-type approach with a Chebyshev polynomial basis for p. Amongst the semi-analytical methods we highlight the work by Koch [4] and Peake [5, 6] both of which essentially take a Wiener–Hopf approach and obtain an approximate solution by the truncation of a large linear system derived from this analysis.

In this paper, we shall make use of the method given in [1], which allows the computation of the amplitudes U_m, D_m, B for an arbitrary choice of blade spacing $s, d > 0$. Specifically, in the numerical examples in §4 of the present manuscript we use the methodology described in [1, §5] and compute the amplitudes from the explicit expressions provided in Eqs. (44) & (45) of that paper.

This solution essentially relies on the Wiener–Hopf analysis of a system of coupled scalar equations and is implemented numerically by solving a truncated representation of an infinite linear system. The original paper [1] contains the full expressions for acoustic waves that are incident from upstream of the cascade and, for completeness, the analogous expressions for downstream incidence can be found in [37, §2.E].

3. An energy balance for the cascade of blades

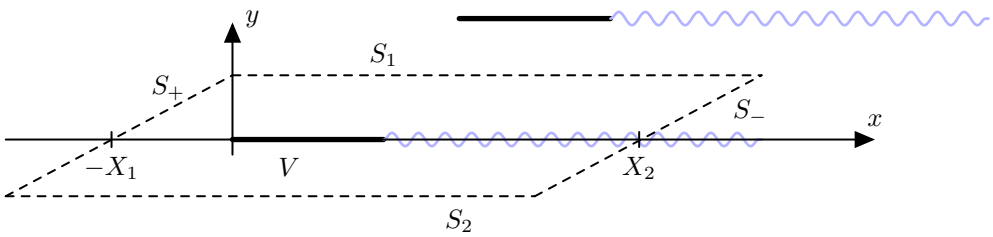

Figure 3: Control volume for the energy balance.

The unsteady velocity field $\mathbf{u}$ can be expressed as the gradient of a potential ϕ which is continuous except for a finite jump across the blades and across the wake downstream of the cascade, so that the unsteady vorticity, in terms of this jump, is

$$\boldsymbol{\omega} = \nabla \times \mathbf{u} = -\hat{\mathbf{z}}\delta(y)\left[\partial_x \phi\right]. \tag{10}$$

For the purpose of describing energy density and flux in this section, we reintroduce a time-dependence in our quantities, such that for instance $\phi = \phi(t, x, y)$. The equation relating the rate of change of acoustic energy, E, to the acoustic energy flux, $\mathbf{I}$, in uniform mean flow $\mathbf{U}$ is well-known and can be found for instance in Goldstein [17, p. 41] (stated here in non-dimensionalised form for an isentropic, source-free flow):

$$\frac{\partial E}{\partial t} + \nabla \cdot \mathbf{I} = \mathbf{u} \cdot (\mathbf{U} \times \boldsymbol{\omega}), \tag{11}$$

where

$$E = \frac{p'\rho'}{2} + \left(\frac{|\mathbf{u}|^2}{2} + \rho' \mathbf{U} \cdot \mathbf{u}\right),$$
$$\mathbf{I} = (p' + \mathbf{U} \cdot \mathbf{u})(\mathbf{u} + \rho' \mathbf{U}),$$

and p', ρ' denote the acoustic pressure and density perturbations. Now consider the domain $V = \{(x, y) \,\big|\, -s/2 < y < s/2, -X_1 + yd/s < x < X_2 + yd/s\}$, as

shown in Fig. 3. Here we take $X_1 > 0, X_2 > 1$. Integrating Eq. (11) over V yields:

$$\frac{\mathrm{d}}{\mathrm{d}t}\int_V E\,\mathrm{d}x + \int_{\partial V} \mathbf{I}\cdot\mathbf{n}\,\mathrm{d}s = \int_V \mathbf{u}\cdot(\mathbf{U}\times\boldsymbol{\omega})\,\mathrm{d}x,$$

and taking a time average one can infer the following balance of energy fluxes for time-harmonic flows:

$$\int_{\partial V} \bar{\mathbf{I}}\cdot\mathbf{n}\,\mathrm{d}s = \int_V \mathbf{u}\cdot(\mathbf{U}\times\boldsymbol{\omega})\,\mathrm{d}x, \tag{12}$$

where on the right hand side the time average $\langle\phi\psi\rangle = \frac{1}{2}\,\mathrm{Re}\,[\phi^*\psi]$ is understood and $\bar{\mathbf{I}}$ denotes the time averaged acoustic energy flux

$$\bar{\mathbf{I}} = \frac{1}{2}\,\mathrm{Re}\left[(p' + \mathbf{U}\cdot\mathbf{u})^*\,(\mathbf{u} + \rho'\mathbf{U})\right]. \tag{13}$$

In Eq. (12) the term on the left hand side represents the time-averaged acoustic energy flux through the boundary ∂V, and the right hand side arises as a consequence of the possibility of energy conversion between the acoustic and vortical unsteady flow and vice versa.

As mentioned in §2 we can derive the correspondence Eq. (2) between direction of the normal to the wavefronts in the incident field, φ, and the physical direction of energy propagation for the incident wave, φ_p, from direct computation of $\bar{\mathbf{I}}$ for the incident plane wave $Ie^{-ik_x x - ik_y y}$ with amplitude I. Indeed we have by Eq. (13)

$$\bar{\mathbf{I}} = \frac{1}{2}\Omega|I|^2\frac{\Omega M(1+2M\cos\varphi+M^2)^{\frac{1}{2}}}{1+M\cos\varphi}\widehat{\mathbf{k}}_p \tag{14}$$

where

$$\widehat{\mathbf{k}}_p = \left(\frac{\cos\varphi + M}{(1+2M\cos\varphi+M^2)^{\frac{1}{2}}}, \frac{\sin\varphi}{(1+2M\cos\varphi+M^2)^{\frac{1}{2}}}\right) = (\cos\varphi_p, \sin\varphi_p). \tag{15}$$

3.1. Interpretations of the interaction term

Before moving on to providing an explicit expression of this energy balance in terms of the modal amplitudes, let us outline a few possible ways to interpret the energy exchange term appearing on the right hand side of Eq. (12) in the context of the relevant literature. For this section we return to considering time-dependent quantities.

Interpretation 1: Rate of work done by a lift force

Howe [25] and Guo [31, p. 191] interpreted the term $\int_V \mathbf{u}\cdot(\mathbf{U}\times\boldsymbol{\omega})\,\mathrm{d}x$ as the rate of work done by the lift force $\mathbf{U}\times\boldsymbol{\omega}$ experienced by vortex elements in the unsteady velocity field of the sound $\mathbf{u}$ (see also [27, p. 407]). The interpretation of the term $\mathbf{U}\times\boldsymbol{\omega}$ as a lift force is a well-known result introduced by Prandtl [38, Eq. (5)]; see also [39, §3.1].

Interpretation 2: Acoustic energy flux into the wake

An alternative interpretation was provided by Rienstra [29, 28]: Let us consider two surfaces $\mathcal{W}_\pm := \{(x,y) \,|\, x > 0, y = 0^\pm\}$ just above/below the wake respectively (i.e. just above/below the faint wavy curves in Fig. 3). Then the acoustic energy flux into the region enclosed by those two curves (i.e. into the wake) is given by

$$\begin{aligned}\int_{\mathcal{W}_-+\mathcal{W}_+} \bar{\mathbf{I}}\cdot\mathbf{n}\,\mathrm{d}s &= -\int_1^\infty (p+\mathbf{U}\cdot\mathbf{u})(\mathbf{u}+\rho\mathbf{U})\Big|_{y=0^+}\cdot\hat{\mathbf{y}}\,\mathrm{d}s \\ &\quad + \int_1^\infty (p+\mathbf{U}\cdot\mathbf{u})(\mathbf{u}+\rho\mathbf{U})\Big|_{y=0^-}\cdot\hat{\mathbf{y}}\,\mathrm{d}s \\ &= -\int_1^\infty [p+\partial_x\phi]\,\partial_y\phi\,\mathrm{d}s \\ &= -\int_1^\infty [\partial_x\phi]\,\partial_y\phi\,\mathrm{d}s,\end{aligned}$$

where $\hat{\mathbf{y}} = (0,1)$. We also have using Eq. (10), $-\int_V \mathbf{u}\cdot(\mathbf{U}\times\boldsymbol{\omega})\,\mathrm{d}x = -\int_1^\infty [\partial_x\phi]\,\mathbf{n}\cdot\boldsymbol{\nabla}\phi\,\mathrm{d}s$. Thus we find

$$-\int_V \mathbf{u}\cdot(\mathbf{U}\times\boldsymbol{\omega})\,\mathrm{d}x = \int_{\mathcal{W}_-+\mathcal{W}_+} \bar{\mathbf{I}}\cdot\mathbf{n}\,\mathrm{d}s,$$

i.e. the energy exchange term can be regarded as the acoustic energy flux into the wake.

Interpretation 3: Change of kinetic energy in the vortical field

This interpretation was given by Howe [26]: Let us focus on the downstream part of the domain, $s(x-1) > dy$, define the vortical component of the field $\mathbf{v} := \boldsymbol{\nabla}\phi_v$, where

$$\phi_v(x,y) = \mathrm{e}^{-\mathrm{i}\,\Omega x} g(y), \quad g(y) = \frac{\mathrm{e}^{\mathrm{i}\,\sigma+\mathrm{i}\,d\Omega}\cosh(\Omega y) - \cosh(\Omega(s-y))}{2(\cos(\sigma+d\Omega)-\cosh(s\Omega))},$$

and denote by ϕ_a the velocity potential of the strictly acoustic contributions (i.e. the modal contributions from $\sigma_m^\pm$ as shown in Tab. 1, whose velocity is continuous everywhere), such that $\mathbf{u} = \boldsymbol{\nabla}\phi_a + \mathbf{v}$. We can write the linearised momentum equation in the form

$$\partial_t\mathbf{v} + \boldsymbol{\nabla}\left(\partial_t\phi_a + p + \mathbf{U}\cdot(\mathbf{v}+\boldsymbol{\nabla}\phi_a)\right) = -\boldsymbol{\omega}\times\left(\mathbf{U}+\mathbf{v}+\boldsymbol{\nabla}\phi_a\right).$$

Taking the dot product of both sides with $\mathbf{U}+\mathbf{v}$ gives to second order

$$\begin{aligned}\frac{1}{2}\partial_t|\mathbf{v}|^2 + \mathbf{v}\cdot\boldsymbol{\nabla}\left(\partial_t\phi_a + p + \mathbf{U}\cdot(\mathbf{v}+\boldsymbol{\nabla}\phi_a)\right) &= -\mathbf{v}\cdot(\boldsymbol{\omega}\times\mathbf{U}) - \mathbf{U}\cdot(\boldsymbol{\omega}\times\mathbf{u}) \\ &= -\boldsymbol{\nabla}\phi_a\cdot(\mathbf{U}\times\boldsymbol{\omega}).\end{aligned}$$

Integration over $\widetilde{V} = \{(x,y) \,\big|\, -s/2 < y < s/2, 1 + yd/s < x < X_2 + yd/s\}$ and using the divergence theorem with the observation that $\boldsymbol{\nabla} \cdot \mathbf{v} = 0$ we find

$$\begin{aligned}\int_{\widetilde{V}} \mathbf{v} \cdot \boldsymbol{\nabla} \left(\partial_t \phi_a + p + \mathbf{U} \cdot (\mathbf{v} + \boldsymbol{\nabla}\phi_a)\right) \mathrm{d}x &= \int_{\partial\widetilde{V}} (\mathbf{n} \cdot \mathbf{v}) \left(\partial_t \phi_a + p + \mathbf{U} \cdot (\mathbf{v} + \boldsymbol{\nabla}\phi_a)\right) \mathrm{d}s \\ &= \int_{\partial\widetilde{V}} (\mathbf{n} \cdot \mathbf{v}) \left(\partial_t \phi_a + p + \mathbf{U} \cdot \mathbf{u}\right) \mathrm{d}s \\ &= \int_{\partial\widetilde{V}} \mathbf{n} \cdot \mathbf{I}_v \, \mathrm{d}s,\end{aligned}$$

where $\mathbf{I}_v = (\mathbf{U} \cdot \mathbf{v})\,\mathbf{v}$ is the energy flux of the vortical field. Therefore the rate of change of vortical kinetic energy in $\widetilde{V}$ can be expressed as

$$\frac{\mathrm{d}}{\mathrm{d}t} \int_V \frac{1}{2} |\mathbf{v}|^2 \, \mathrm{d}x = \underbrace{-\int_{\partial\widetilde{V}} \mathbf{n} \cdot \mathbf{I}_v \, \mathrm{d}s}_{\text{flux of vortical energy out of } \widetilde{V}} \qquad \underbrace{-\int_{\widetilde{V}} \boldsymbol{\nabla}\phi_a \cdot (\mathbf{U} \times \boldsymbol{\omega}) \, \mathrm{d}x}_{\text{exchange of energy with acoustic field}} \quad .$$

Relationship to interface flux

As a final interpretation we note that we can also relate the energy exchange term on the right hand side of Eq. (12) directly to the *interface flux* that is described by Arzoumanian [32] for a vortex sheet in an incompressible fluid (and which also occurs when two fluid layers are separated by an elastic sheet as described in [33]). Indeed, in reality, the vortex sheets are located at a small displacement $y = \eta(t,x)$, which is to ensure they are convected with the flow (zero flow across the wake):

$$\frac{\mathrm{D}\eta}{\mathrm{D}t} = \partial_y \phi.$$

Furthermore, the form of the discontinuity in ϕ is fixed to ensure continuity of pressure (cf. [40]) such that

$$-\frac{\mathrm{D}\,[\phi]}{\mathrm{D}t} = [p] = 0.$$

We can combine these two observations to show (after a few steps of algebra):

$$\begin{aligned}\int_V \mathbf{u} \cdot (\mathbf{U} \times \boldsymbol{\omega}) \, \mathrm{d}x &= \int_V \mathbf{u} \cdot \hat{\boldsymbol{y}} \delta(y) \, [\partial_x \phi] \, \mathrm{d}x \\ &= \frac{\mathrm{d}}{\mathrm{d}t} \int_1^{X_2} \eta \, [\partial_x \phi] \, \mathrm{d}s - J_i(X_2) + J_i(1),\end{aligned}$$

where $J_i(x) = \eta \, [\partial_t \phi]$. We note that the wake is attached to the blades at the trailing edges, $\eta(1) = 0$, thus $J_i(1) = 0$. Taking a time average ensures that, in our time-harmonic flow, the contribution from $\frac{\mathrm{d}}{\mathrm{d}t} \int_1^{X_2} \eta \, [\partial_x \phi] \, \mathrm{d}s$ vanishes. This allows us to conclude that the time-average of the right hand side in Eq. (12) is $-J_i(X_2)$, which is precisely the expression for the interface flux described by Arzoumanian [32] (given here in non-dimensionalised form), and the analogue for a vortex sheet of the definition by Crighton & Oswell [33].

3.2. Time-averaged energy balance in terms of amplitudes

We can now return to Eq. (12) and provide explicit expressions for the energy fluxes in terms of the modal amplitudes of the velocity potential. Noting the continuity of the velocity potential across S_1, S_2 we observe that in Eq. (12) the contributions from S_1 and S_2 cancel. Moreover, on the blade we have $\partial\phi/\partial y = 0$ so the contribution from this part of ∂V is zero, and the left hand side of Eq. (12) reduces to an integral over S_+ and S_-.

Let us now focus on the time-harmonic case and take the usual time-average. By the expressions for the far-field from §2.1 we have only acoustic contributions to $\int_{S_+}$ and acoustic mixed with hydrodynamic contributions to $\int_{S_-}$. Of course, the evanescent (cut-off) acoustic modes carry zero energy. The interaction of all the downstream acoustic modes σ_m^- with the hydrodynamic mode will, in general, involve contributions proportional to $\exp(\mathrm{i}((\sigma_m^-)^* - \Omega)X_2)$. These contributions cancel with terms from $\int_V \mathbf{u}\cdot(\mathbf{U}\times\boldsymbol{\omega})\,\mathrm{d}x$. To see this let us demonstrate the idea based on the special case when we have upstream incidence and $d = 0$ (this is such that the algebraic expressions remain within reasonable simplicity): Here the contribution from $\int_{S_-}$ takes the form

$$\begin{aligned}
\int_{S_-} \bar{\mathbf{I}}\cdot\mathbf{n}\,\mathrm{d}s &= \frac{1}{2}\,\mathrm{Re}\left[\int_0^s (-\mathrm{i}\,\Omega\phi(X_2,y))^*\left(\beta^2\partial_x\phi(X_2,y) - \mathrm{i}\,\Omega M^2\phi(X_2,y)\right)\mathrm{d}y\right] \\
&= \frac{1}{2}\,\mathrm{Re}\left[\mathrm{i}\,\Omega\int_0^s \left(B^*\mathrm{e}^{\mathrm{i}\,\Omega X_2}g^*(y) + \sum_{m\in\mathbb{Z}} D_m^*\mathrm{e}^{\mathrm{i}(\sigma_m^-)^*X_2}\mathrm{e}^{\gamma(\sigma_m^-)^*y}\right)\right. \\
&\qquad \left(B\mathrm{e}^{-\mathrm{i}\,\Omega X_2}(-\mathrm{i}\,\beta^2\Omega - i\Omega M^2)g(y)\right. \\
&\qquad\quad \left.\left. + \sum_{m\in\mathbb{Z}} D_m\mathrm{e}^{-\mathrm{i}\,\sigma_m^-X_2}\mathrm{e}^{\gamma(\sigma_m^-)y}\left(-\mathrm{i}\,\sigma_m^-\beta^2 - \mathrm{i}\,\Omega M^2\right)\right)\mathrm{d}y\right]
\end{aligned}$$

The contribution from terms involving both the hydrodynamic and acoustic modes are thus

$$\begin{aligned}
&\frac{1}{2}\,\mathrm{Re}\left[\mathrm{i}\,\Omega\int_0^s \left(\sum_{m\in\mathbb{Z}} D_m^*\mathrm{e}^{\mathrm{i}(\sigma_m^-)^*X_2}B\mathrm{e}^{-\mathrm{i}\,\Omega X_2}\mathrm{e}^{\gamma(\sigma_m^-)^*y}g(y)\right)\right. \\
&\qquad\qquad \left.\left(-i\beta^2\Omega - \mathrm{i}\,\Omega M^2 - \mathrm{i}(\sigma_m^-)^*\beta^2 - \mathrm{i}\,\Omega M^2\right)\mathrm{d}y\right] \\
&= \frac{1}{2}\,\mathrm{Re}\left[-\mathrm{i}\,\Omega\sum_{m\in\mathbb{Z}} D_m^*\mathrm{e}^{\mathrm{i}(\sigma_m^-)^*X_2}B\mathrm{e}^{-\mathrm{i}\,\Omega X_2}\right. \\
&\qquad\qquad \left.\left(\mathrm{i}\,\beta^2\Omega + 2\,\mathrm{i}\,\Omega M^2 + \mathrm{i}(\sigma_m^-)^*\beta^2\right)\int_0^1 \mathrm{e}^{\gamma(\sigma_m^-)^*y}g(y)\,\mathrm{d}y\right]
\end{aligned}$$

Using Eq. (9) we find

$$\int_0^s \mathrm{e}^{\gamma(\sigma_m^-)^*\tilde{y}} g(y)\,\mathrm{d}y = \int_0^s \frac{\mathrm{e}^{\gamma(\sigma_m^-)^* y}\mathrm{e}^{\mathrm{i}\,\sigma}\cosh(\Omega y) - \mathrm{e}^{\gamma(\sigma_m^-)^* y}\cosh(\Omega(s-y))}{2(\cos\sigma - \cosh(s\Omega))}\,\mathrm{d}y$$
$$= -\frac{\gamma^*(\sigma_m^-)}{(\gamma^*(\sigma_m^-))^2 - \Omega^2}$$

where we used $s\gamma(\sigma_m^-)^* = -\mathrm{i}\,\sigma - 2\pi\,\mathrm{i}\,m$. Thus the contribution from terms involving both the hydrodynamic and acoustic modes equals

$$\frac{1}{2}\,\mathrm{Re}\left[-\mathrm{i}\,\Omega\sum_{m\in\mathbb{Z}} D_m^*\mathrm{e}^{\mathrm{i}(\sigma_m^-)^* X_2} B\mathrm{e}^{-\mathrm{i}\,\Omega X_2}\gamma^*(\sigma_m^-)\frac{\left(-\mathrm{i}\,\beta^2\Omega - 2\,\mathrm{i}\,\Omega M^2 - \mathrm{i}(\sigma_m^-)^*\beta^2\right)}{((\sigma_m^-)^*)^2\beta^2 + 2(\sigma_m^-)^* M^2\Omega - \Omega^2(1+M^2)}\right]$$
$$= \frac{1}{2}\,\mathrm{Re}\left[-\mathrm{i}\,\Omega\sum_{m\in\mathbb{Z}} D_m^* B\mathrm{e}^{\mathrm{i}(\sigma_m^-)^* X_2}\mathrm{e}^{-\mathrm{i}\,\Omega X_2}\frac{\gamma^*(\sigma_m^-)}{\mathrm{i}(\sigma_m^-)^* - \mathrm{i}\,\Omega}\right]$$

In this special case the integral $\int_V \mathbf{u}\cdot(\mathbf{U}\times\boldsymbol{\omega})\,\mathrm{d}x$, takes the form

$$\int_V \mathbf{u}\cdot(\mathbf{U}\times\boldsymbol{\omega})\,\mathrm{d}x = \frac{1}{2}\,\mathrm{Re}\int_1^{X_2}\partial_y\phi(x,0)^*[\partial_x\phi](x)\,\mathrm{d}x$$
$$= \frac{1}{2}\,\mathrm{Re}\left[-\mathrm{i}\,\Omega\int_1^{X_2}\left(B\mathrm{e}^{-\mathrm{i}\,\Omega x}\Omega\frac{\sinh(s\Omega)}{2(\cos(\sigma+d\Omega)-\cosh(s\Omega))}\right.\right.$$
$$\left.\left. + \sum_{m\in\mathbb{Z}} D_m\gamma(\sigma_m^-)\mathrm{e}^{-\mathrm{i}\,\sigma_m^- x}\right)^* B\mathrm{e}^{-\mathrm{i}\,\Omega x}\,\mathrm{d}x\right]$$
$$= \frac{1}{2}\,\mathrm{Re}\left[-\mathrm{i}\,\Omega\int_1^{X_2}\sum_{m\in\mathbb{Z}} D_m^* B\gamma(\sigma_m^-)^*\mathrm{e}^{(\mathrm{i}(\sigma_m^-)^* - \mathrm{i}\,\Omega)x}\,\mathrm{d}x\right]$$
$$= \frac{1}{2}\,\mathrm{Re}\left[-\mathrm{i}\,\Omega\sum_{m\in\mathbb{Z}} D_m^* B\gamma(\sigma_m^-)^*\frac{\mathrm{e}^{(\mathrm{i}(\sigma_m^-)^* - \mathrm{i}\,\Omega)X_2} - \mathrm{e}^{\mathrm{i}(\sigma_m^-)^* - \mathrm{i}\,\Omega}}{\mathrm{i}(\sigma_m^-)^* - \mathrm{i}\,\Omega}\right] \tag{16}$$

Thus one can see that any terms involving $\exp\left(\mathrm{i}((\sigma_m^-)^* - \Omega)X_2\right)$ cancel exactly in Eq. (12). This remains true for downstream incidence and when $d \neq 0$ (though the algebra is more tedious) and it is therefore possible, for any fixed $X_1 > 0, X_2 > 1$, to arrive at an *exact energy balance* in terms of the modal amplitudes which is *independent* of X_1, X_2:

$$P_I = P_U + P_D + P_H + \Pi_\omega, \tag{17}$$

where in the above P_U, P_D are the acoustic sound powers that are radiated to $x = \pm\infty$ respectively and P_I is the sound power of the incoming wave. Furthermore, P_H is the power carried by the hydrodynamic mode to $x = +\infty$ and Π_ω is the energy conversion term due to the lift force experienced by particles on the vortex sheet, arising from the right hand side of equation Eq. (12). After

a few steps of algebra we find the following explicit expressions in terms of the amplitudes, where the aforementioned cancelling contributions proportional to $\exp\left(\mathrm{i}((\sigma_m^-)^* - \Omega)X_2\right)$ have been dropped (this is also equivalent to taking an average over $X_2 \in (1,\infty)$ in the sense $\langle \Pi_\omega \rangle = \lim_{L\to\infty} L^{-1} \int_0^L \Pi_\omega \,\mathrm{d}X_2$ *using the expression Eq.* (16)):

$$
\begin{aligned}
P_U &= -\frac{\Omega}{2} \sum_{-r\le m\le q} |U_m|^2 (s\Omega M^2 + s\beta^2\sigma_m^+ - d\gamma(\sigma_m^+)),\\
P_D &= \frac{\Omega}{2} \sum_{-r\le m\le q} |D_m|^2 (-s\Omega M^2 - s\beta^2\sigma_m^- - d\gamma(\sigma_m^-)),\\
P_I &= \begin{cases} \frac{\Omega}{2}|I|^2(-s\Omega M^2 - s\beta^2\sigma_0^- - d\gamma(\sigma_0^-)), & \text{if } k_x = \sigma_0^-,\\ \frac{\Omega}{2}|I|^2(-s\Omega M^2 - s\beta^2\sigma_0^+ + d\gamma(\sigma_0^+)), & \text{if } k_x = \sigma_0^+, \end{cases}
\end{aligned}
\tag{18}
$$

where $r, q \in \mathbb{N}$ are such that a mode $\sigma_m^\pm$ is cut-on (i.e. propagating to $x = \mp\infty$) if and only if $-r \le m \le q$ (cf. §2.1). Furthermore,

$$
\begin{aligned}
P_H &= \frac{\Omega}{2}|B|^2 \left(s\Omega \int_0^1 |g(st)|^2 \,\mathrm{d}t + \mathrm{Im}\left[d \int_0^1 g(st)^* g'(st) \,\mathrm{d}t \right] \right)\\
&= \frac{\Omega|B|^2}{8(\cos(\sigma + d\Omega) - \cosh(\Omega))^2}\\
&\quad \Big(\frac{\Omega s + \cosh(\Omega s)\sinh(\Omega s) - \cos(\sigma + d\Omega)(\Omega s\cosh(\Omega s) + \sinh(\Omega s))}{\Omega s}\\
&\qquad - \Omega d \sin(\sigma + d\Omega)\sinh(\Omega s) \Big),
\end{aligned}
$$

and finally,

$$
\Pi_\omega = -\frac{\Omega}{2}\,\mathrm{Im}\left[\sum_{m\in\mathbb{Z}} B^* D_m \gamma(\sigma_m^-) \frac{\mathrm{e}^{\mathrm{i}\Omega - \mathrm{i}\sigma_m^-}}{\mathrm{i}\Omega - \mathrm{i}\sigma_m^-} + \begin{cases} 0, & \text{if } k_x = \sigma_0^-\\ -B^* I \gamma(\sigma_0^+) \frac{\mathrm{e}^{\mathrm{i}\Omega - \mathrm{i}\sigma_0^+}}{\mathrm{i}\Omega - \mathrm{i}\sigma_0^+}, & \text{if } k_x = \sigma_0^+ \end{cases} \right].
$$

The decomposition of outgoing energy flux into acoustic and hydrodynamic contributions, and the sound power absorbed by the wake as can be seen on the left hand side of Eq. (17) is analogous to the power decomposition for acoustic scattering on a semi-infinite annular duct in subsonic mean flow given by Rienstra [28, §6].

4. Results and discussion

As mentioned above the following numerical results were produced using the methodology given in [1, §5]. Specifically, the explicit expressions for the amplitudes U_m, D_m, B in the case of upstream incidence can be found in Eqs. (44) & (45) of this paper, and the corresponding expressions for downstream incidence are provided in [37, §2.E].

4.1. Symmetries in the field and zero acoustic reflection

We begin by considering the amplitudes of the first radiating modes U_0, D_0 for various values of φ. In Figs. 4-5 & 8-9 we have plotted these amplitudes as a function of φ. In these graphs we choose $\alpha_0 = \pi/6, d^2 + s^2 = 1$, and $\Omega M = \pi/4, 5\pi/4$ respectively, such that the parameters for the two figures differ only in reduced frequency and hence in the number of cut-on acoustic modes. In particular in Figs. 4-5 only $\sigma_0^{\pm}$ are cut-on, whereas in Figs. 8-9 the cut-on acoustic modes are $\sigma_0^{\pm}, \sigma_{-1}^{\pm}$.

In order to allow for comparison against earlier work by Koch [4] we plot the modal pressures defined as follows:

$$P_0^i = \begin{cases} (-\mathrm{i})(\Omega - \sigma_0^-)I, & \text{if } k_x = \sigma_0^-, \\ (-\mathrm{i})(\Omega - \sigma_0^+)I, & \text{if } k_x = \sigma_0^+, \end{cases}$$

$$P_0^t = \begin{cases} (-\mathrm{i})(\Omega - \sigma_0^-)D_0, & \text{if } k_x = \sigma_0^-, \\ (-\mathrm{i})(\Omega - \sigma_0^+)U_0, & \text{if } k_x = \sigma_0^+, \end{cases} \quad P_0^r = \begin{cases} (-\mathrm{i})(\Omega - \sigma_0^+)U_0, & \text{if } k_x = \sigma_0^-, \\ (-\mathrm{i})(\Omega - \sigma_0^-)D_0, & \text{if } k_x = \sigma_0^+. \end{cases}$$

In Figs. 4-5 & 8-9 the transition from upstream to downstream incidence and vice versa is marked with ■ and ▲ respectively (solid, left-half-filled and right-half-filled shapes correspond to $M = 0.0, 0.3$ and 0.7 respectively), such that for each value of M the wave is downstream incident if $\varphi - \alpha_0$ is between ■ and ▲. Note the region of upstream incidence is fixed by the condition $M \sin\alpha_0 + \sin(\alpha_0 - \varphi) > 0$ (see [1, §3.1.1]). Due to convection, larger values of M result in a wider range of values for $\varphi - \alpha_0$ corresponding to upstream incidence. There are a few interesting features that we can observe in Figs. 4-5 & 8-9:

1. When only $\sigma_0^{\pm}$ are cut-on acoustic modes (as is the case in Figs. 4-5) and we have zero mean flow ($M = 0$), the reflected and transmitted amplitudes are symmetric about $\varphi = \pi + \alpha_0$, i.e. the amplitudes for $\varphi - \alpha_0 = \pi + \beta$ equal in modulus those for $\varphi - \alpha_0 = \pi - \beta$ for any $\beta \in (0, \pi)$. This is in addition to the obvious symmetry between the amplitudes for $\varphi - \alpha_0 = \beta$ and $\varphi - \alpha_0 = \beta + \pi$. The latter is simply due to the fact that for $M = 0$ there is no distinction between upstream incidence and downstream incidence as shown in Fig. 6. However a proof of the former requires slightly more careful consideration as is shown below.
2. For any value of $M \in [0, 1), \Omega \in [0, \infty)$ the cascade is perfectly transmitting ($|P_0^t|/|P_0^i| = 1$) when $\varphi = 0, \pi$ (the points $\varphi - \alpha_0 = 330°$ and $\varphi - \alpha_0 = 150°$ respectively), corresponding to incident waves from upstream and downstream respectively propagating perfectly parallel to, and therefore being unimpeded by, the blades.
3. For any choice of M and Ω there are two *additional points of zero acoustic reflection* ($|P_0^r|/|P_0^i| = 0$), marked with ▼ and ● in Figs. 5 & 9. When $M = 0$ these are located at $\varphi = \alpha_0, \pi + \alpha_0$ and for nonzero M these points shift slightly to increased/decreased values of φ respectively.

These features were observed numerically, for the case of a single cut-on acoustic mode $\sigma_0^{\pm}$, by Koch [4], and studied analytically (in the context of specific metamaterials) for the case of zero mean flow, $M = 0$, by Porter [34].
305 *It turns out that point 1 above is indeed a property of the field as long as only a single cut-on propagating mode exits upstream and downstream of the cascade and in Fig. 8 we see that the symmetry breaks down for the transmitted amplitude when multiple acoustic modes are cut-on. Furthermore, points 2 and 3 are properties of the field for any value of M and Ω.*

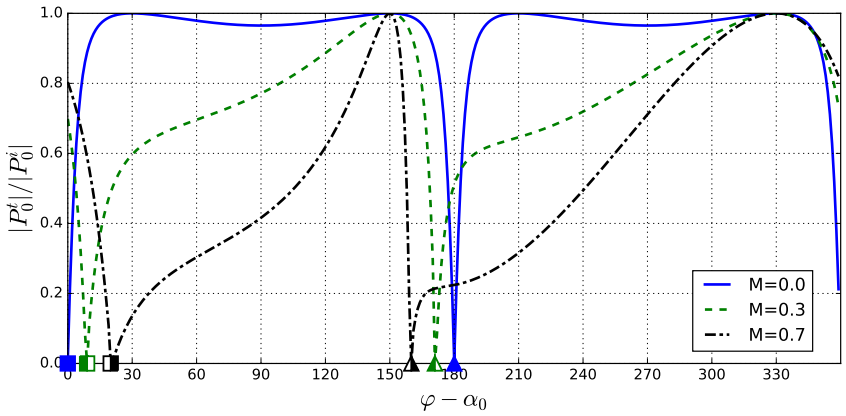

Figure 4: Relative modal pressures of the first transmitted mode ($\alpha_0 = 30°$ and $\Omega M = \pi/4$).

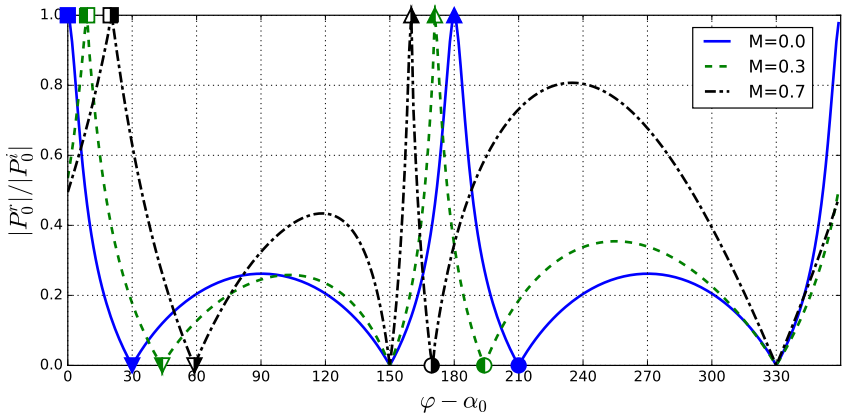

Figure 5: Relative modal pressures of the first reflected mode ($\alpha_0 = 30°$ and $\Omega M = \pi/4$).

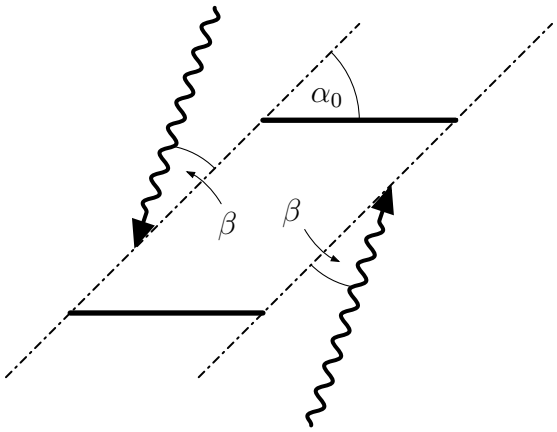

Figure 6: Standard symmetry in the field when $M = 0$.

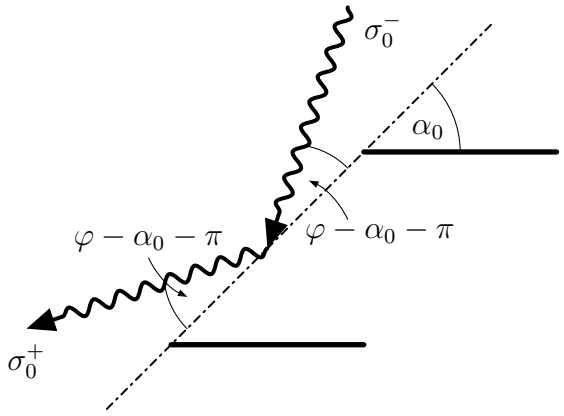

Figure 7: The angles of propagation for $\sigma_0^{\pm}$ $(M = 0)$.

310

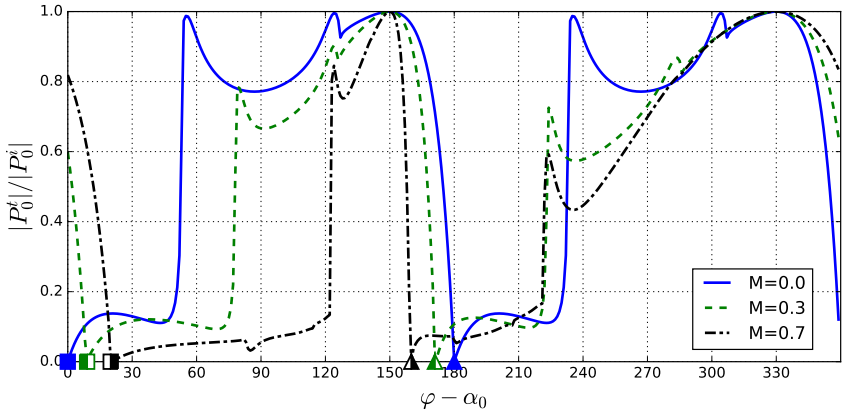

Figure 8: Relative modal pressures of the first transmitted mode ($\alpha_0 = 30°$ and $\Omega M = 5\pi/4$).

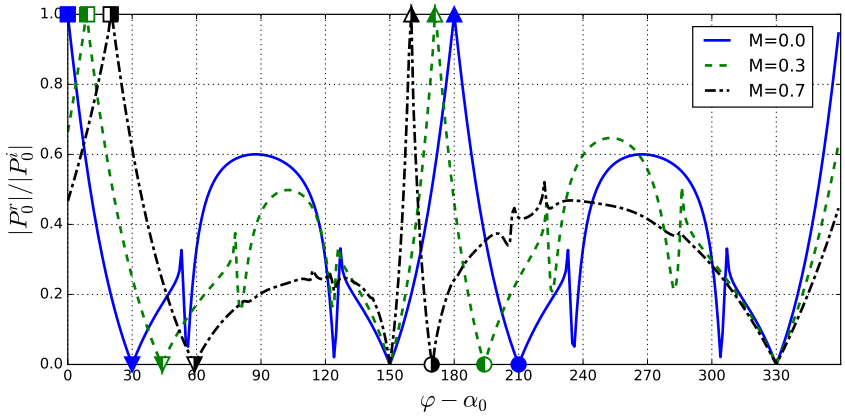

Figure 9: Relative modal pressures of the first reflected mode ($\alpha_0 = 30°$ and $\Omega M = 5\pi/4$).

Of course, it is clear that point 2 must hold since for $\varphi = 0, \pi$ the waves are unimpeded by the blades. In this section we provide a proof of features 1 and 3 based entirely on the energy balance – the underlying idea is that there is a direct correspondence between the cascade response for an incident mode σ_0^- from upstream and the response for an incident mode σ_0^+ from downstream.

To understand this correspondence, we need to relate the angles of propagation of the zeroth radiating modes $\sigma_0^\pm$ more explicitly and for this purpose it is useful to describe the geometry in terms of the stagger angle α_0 and the leading edge separation c such that $s = c\sin\alpha_0, d = c\cos\alpha_0$. This allows us to write the inter-blade phase angle, as defined in Eq. (4), as

$$\sigma = \frac{-\Omega M}{1 + M\cos\varphi} c\cos(\varphi - \alpha_0),$$

and hence the zeroth radiating mode (cf. Eq. (8)) in the form

$$\sigma_0^{\pm} = \frac{M\Omega\left(\cos\varphi(1-M^2\sin^2\alpha_0) - M\sin^2\alpha_0 - \sin\alpha_0\sin(\alpha_0-\varphi)\right)}{(1+M\cos\varphi)\left(1-M^2\sin^2\alpha_0\right)} \mp \frac{M\Omega\sin\alpha_0|M\sin\alpha_0+\sin(\alpha_0-\varphi)|}{(1+M\cos\varphi)\left(1-M^2\sin^2\alpha_0\right)}.$$

As mentioned above, an incident acoustic wave with $k_x = \Omega M\cos\varphi/(1+M\cos\varphi)$ is effectively incident from upstream if and only if $M\sin\alpha_0+\sin(\alpha_0-\varphi) > 0$ (cf . [1, §3.1.1]), and in that case we have

$$\begin{aligned}\sigma_0^- &= \frac{\Omega M\cos\varphi}{1+M\cos\varphi} = k_x,\\ \sigma_0^+ &= \frac{\Omega M\cos\tilde{\varphi}}{1+M\cos\tilde{\varphi}},\end{aligned} \tag{19}$$

where

$$\cos\tilde{\varphi} = \frac{\cos(\varphi-2\alpha_0) - 2M\sin^2\alpha_0 - M^2\cos\varphi\sin^2\alpha_0}{1+2M\sin(\alpha_0-\varphi)\sin\alpha_0+M^2\sin^2\alpha_0}.$$

In the case of zero mean flow the latter expression reduces to $\cos\tilde{\varphi} = \cos(\varphi-2\alpha_0)$. If we have downstream incidence, $M\sin\alpha_0+\sin(\alpha_0-\varphi) < 0$, the expressions for these two modes are reversed. As mentioned earlier the cascade is perfectly transmitting ($|P_0^t|/|P_0^i| = 1, |P_0^r|/|P_0^i| = 0$) when $\varphi = 0, \pi$ due to the incident waves propagating parallel to, and therefore being unimpeded by, the cascade blades. There are two corresponding angles of inclination of the normal to the wavefronts, $\tilde{\varphi}_0, \tilde{\varphi}_\pi$ in the following sense:

- If $\varphi = 0$, then

$$\begin{aligned}\sigma_0^+ &= \frac{\Omega M\cos\tilde{\varphi}_0}{1+M\cos\tilde{\varphi}_0},\\ \cos\tilde{\varphi}_0 &= \frac{\cos(2\alpha_0) - 2M\sin^2\alpha_0 - M^2\sin^2\alpha_0}{1+2M\sin^2\alpha_0+M^2\sin^2\alpha_0},\end{aligned} \tag{20}$$

  and in particular when $M = 0$ we have $\tilde{\varphi}_0 = 2\alpha_0$.

- If $\varphi = \pi$, then

$$\begin{aligned}\sigma_0^- &= \frac{\Omega M\cos\tilde{\varphi}_\pi}{1+M\cos\tilde{\varphi}_\pi},\\ \cos\tilde{\varphi}_\pi &= \frac{\cos(\pi+2\alpha_0) - 2M\sin^2\alpha_0 + M^2\sin^2\alpha_0}{1+2M\sin(\alpha_0-\pi)\sin\alpha_0+M^2\sin^2\alpha_0},\end{aligned} \tag{21}$$

  and in particular when $M = 0$ we have $\tilde{\varphi}_\pi = \pi+2\alpha_0$.

This means that σ_0^+ has a direction of propagation as if it was reflected directly on the cascade front (cf. sketch for $M = 0$ in Fig. 7). So in a sense $\sigma_0^\pm$ are the usual plane wave modes that one would expect to find for reflection on a flat material that is located parallel to the cascade front.

Symmetry along the cascade face in zero mean flow

We now show the symmetry of the transmission and reflection amplitudes with respect to $\varphi - \alpha_0 = \pi$ in the case of zero mean flow, i.e. property 1 as described above. As can be seen from Fig. 8 this symmetry is no longer true for the transmitted amplitude if there is more than a single propagating wave mode upstream and downstream of the cascade. Thus in this section we focus on the case when only $\sigma_0^{\pm}$ are cut-on. Let $\varphi = \pi + \alpha_0 + \beta$ and $\tilde{\varphi} = \pi + \alpha_0 - \beta$ for some $\beta > 0$. Then the cascade response for an incident field with normal to the wavefronts that is inclined at an angle φ is

$$\phi_1(x,y) = \begin{cases} I\mathrm{e}^{-\mathrm{i}\sigma_0^- x}\mathrm{e}^{\gamma(\sigma_0^-)y} + R_1\mathrm{e}^{-\mathrm{i}\sigma_0^+ x}\mathrm{e}^{\gamma(\sigma_0^+)y} + \text{cut-off modes}, & sx < dy, \\ T_1\mathrm{e}^{-\mathrm{i}\sigma_0^- x}\mathrm{e}^{\gamma(\sigma_0^-)y} + \text{cut-off modes}, & sx > dy + 1. \end{cases}$$

and the response for an incident field with normal to the wavefronts that is inclined at an angle $\tilde{\varphi}$ is (according to Eq. (19) the radiating modes are the same: $\sigma_0^{\pm}(\varphi) = \sigma_0^{\pm}(\tilde{\varphi})$)

$$\phi_2(x,y) = \begin{cases} T_2\mathrm{e}^{-\mathrm{i}\sigma_0^+ x}\mathrm{e}^{\gamma(\sigma_0^+)y} + \text{cut-off modes}, & sx < dy, \\ I\mathrm{e}^{-\mathrm{i}\sigma_0^+ x}\mathrm{e}^{\gamma(\sigma_0^+)y} + R_2\mathrm{e}^{-\mathrm{i}\sigma_0^- x}\mathrm{e}^{\gamma(\sigma_0^-)y} + \text{cut-off modes}, & sx > dy + 1. \end{cases}$$

By linearity we can add the two fields to produce a valid solution of the scattering problem of the following form (for any arbitrary $z \in \mathbb{C}$):

$$\phi_1 + z\phi_2 = \begin{cases} zI\mathrm{e}^{-\mathrm{i}\sigma_0^- x}\mathrm{e}^{\gamma(\sigma_0^-)y} + (R_1 + zT_2)\mathrm{e}^{-\mathrm{i}\sigma_0^+ x}\mathrm{e}^{\gamma(\sigma_0^+)y} + \text{cut-off modes}, & sx < dy, \\ I\mathrm{e}^{-\mathrm{i}\sigma_0^+ x}\mathrm{e}^{\gamma(\sigma_0^+)y} + (T_1 + zR_2)\mathrm{e}^{-\mathrm{i}\sigma_0^- x}\mathrm{e}^{\gamma(\sigma_0^-)y} + \text{cut-off modes}, & sx > dy + 1. \end{cases}$$

This field must satisfy the original equation of motion, and thus the time-averaged energy balance must remain valid (in this case however we have both upstream and downstream contribution from the incident wave):

$$|I|^2 + |zI|^2 = |R_1 + zT_2|^2 + |T_1 + zR_2|^2, \quad \forall z \in \mathbb{C}. \tag{22}$$

Taking $z \to 0, \infty$ respectively yields

$$|I|^2 = |T_1|^2 + |R_1|^2 = |T_2|^2 + |R_2|^2. \tag{23}$$

We can simplify Eq. (22) using Eq. (23) to find

$$\mathrm{Re}\left[zR_1^* T_2\right] = -\mathrm{Re}\left[zT_1^* R_2\right], \quad \forall z \in \mathbb{C}.$$

Since this holds for all values of $z \in \mathbb{C}$ we infer that $R_1^* T_2 = T_1^* R_2$ which, together with Eq. (23), proves $|R_1| = |R_2|, |T_1| = |T_2|$, i.e. transmission and reflection amplitudes are symmetric with respect to $\varphi - \alpha_0 = \pi$.

Zero acoustic reflection in leading radiating mode for subsonic mean flow

Although this aforementioned symmetry is not preserved in the case when $M > 0$, we still find two special angles of inclination of the normal to the wavefronts, $\tilde{\varphi}_0, \tilde{\varphi}_\pi$ as defined in Eqs. (20) & (21), for which the reflected acoustic field

has zero contribution from the zeroth radiating mode (and hence is identically zero in the far-field when there is only one cut-on mode). *Note this property holds irrespective of the number of cut-on modes in the field.* These special angles are marked in Figs. 5, 9 & 10, with ▼ and ● corresponding to $\tilde{\varphi}_0$ and $\tilde{\varphi}_\pi$ respectively. As can be seen from Fig. 10, when $M > 0$, there may be a nonzero contribution from the hydrodynamic mode (which is part of the reflected field in the case $\tilde{\varphi}_0$).

We focus on the case $\tilde{\varphi}_0$ (i.e. downstream incidence) since the case $\tilde{\varphi}_\pi$ can be treated analogously: Let the total velocity potential due to an incident wave with normal to the wavefronts inclined at an angle $\tilde{\varphi}_0$ be denoted by

$$\tilde{\phi}(x,y) = \begin{cases} \sum_{m\in\mathbb{Z}} T_m \mathrm{e}^{-\mathrm{i}\,\sigma_m^+ x}\mathrm{e}^{-\mathrm{i}\,\gamma(\sigma_m^+)y}, & sx < dy, \\ I\mathrm{e}^{-\mathrm{i}\,\sigma_0^+ x}\mathrm{e}^{-\gamma(\sigma_0^+)y} + B\mathrm{e}^{-\mathrm{i}\,\Omega x}g(y) + \sum_{m\in\mathbb{Z}} R_m \mathrm{e}^{-\mathrm{i}\,\sigma_m^- x}\mathrm{e}^{\gamma(\sigma_m^-)y}, & sx > dy + 1. \end{cases}$$

We know from our prior discussion that the mode $\sigma_0^- = \sigma_0^-(\tilde{\varphi}_0) = \sigma_0^-(0)$ corresponds to the angle $\varphi = 0$ and that the response for this type of parallel-propagating mode must be of the form

$$\phi(x,y) = I\mathrm{e}^{-\mathrm{i}\,\sigma_0^- x}\mathrm{e}^{-\mathrm{i}\,\gamma(\sigma_0^-)y} = I\mathrm{e}^{-\mathrm{i}\,\sigma_0^- x}, \quad (x,y) \in \mathbb{R}^2.$$

As for the zero mean flow case, we consider the superposition of these two fields, $\tilde{\phi} + z\phi$, which is a valid solution to the scattering problem and hence satisfies the time-averaged energy balance (which must again account for incident fields both upstream and downstream of the cascade):

$$P_U + P_D + P_H + \Pi_\omega = P_I, \tag{24}$$

where

$$\begin{aligned}
P_U &= -\sum_{-r\le m\le q} |T_m|^2(s\Omega M^2\beta^{-1} + s\beta\sigma_m^+ - d\beta^{-1}\gamma(\sigma_m^+)) \\
P_D &= |R_0 + zI|^2(-s\Omega M^2\beta^{-1} - s\beta\sigma_0^- - d\beta^{-1}\gamma(\sigma_0^-)) \\
&\quad + \sum_{-r\le m\le q} |R_m|^2(-s\Omega M^2\beta^{-1} - s\beta\sigma_m^- - d\beta^{-1}\gamma(\sigma_m^-)) \\
P_I &= |zI|^2(-s\Omega M^2\beta^{-1} - s\beta\sigma_0^- - d\beta^{-1}\gamma(\sigma_0^-)) + |I|^2(-s\Omega M^2\beta^{-1} - s\beta\sigma_0^+ + d\beta^{-1}\gamma(\sigma_0^+)) \\
P_H &= |B|^2\left(s\Omega\beta^{-1}\int_0^1 |g(st)|^2\,\mathrm{d}t + \mathrm{Im}\left[\beta^{-1}d\int_0^1 g(st)^* g'(st)\,\mathrm{d}t\right]\right) \\
\Pi_\omega &= -\,\mathrm{Im}\left[B^*(zI + R_0)\gamma(\sigma_0^-)\frac{\mathrm{e}^{\mathrm{i}\,\Omega - i\sigma_0^-}}{\mathrm{i}\,\Omega\beta - \mathrm{i}\,\beta\sigma_0^-} - B^* I\gamma(\sigma_0^+)\frac{\mathrm{e}^{\mathrm{i}\,\Omega - \mathrm{i}\,\sigma_0^+}}{\mathrm{i}\,\Omega\beta - \mathrm{i}\,\beta\sigma_0^+}\right. \\
&\qquad \left. + \sum_{m\in\mathbb{Z}, m\neq 0} B^* R_m\gamma(\sigma_m^-)\frac{\mathrm{e}^{\mathrm{i}\,\Omega - \mathrm{i}\,\sigma_m^-}}{\mathrm{i}\,\Omega\beta - \mathrm{i}\,\beta\sigma_m^-}\right].
\end{aligned}$$

One can quickly check that in the current case $\gamma(\sigma_0^-) = 0$, and hence by setting $z \to 0, +\infty$ and using the resulting equations to cancel appropriate terms in

Eq. (24), we arrive at

$$\mathrm{Re}\left[R_0^* z I\right]\left(-s\Omega M^2\beta^{-1} - s\beta\sigma_0^-\right) = 0 \quad \forall z \in \mathbb{C},$$

which implies $R_0 = 0$, i.e. the leading radiating mode σ_0^- has zero contribution to the reflected far-field. Of course, in general, the remaining reflected amplitudes, R_m with $m \neq 0$, need not vanish when $\varphi = \tilde{\varphi}_0$ or $\varphi = \tilde{\varphi}_\pi$, i.e. sound may be scattered into higher order reflected modes. Thus, while $R_0 = 0$ holds regardless of the choice of frequency and subsonic mean-flow speed, the reflected sound power is truly zero only when a single acoustic mode is cut-on.

4.2. The significance of the hydrodynamic and energy conversion terms in balancing the energy

We now visualise the terms from the time-averaged energy balance Eq. (17), to understand their individual contribution to the overall outgoing power. In order to facilitate comparison against the amplitudes shown in Figs. 4-5 we plot here (and also in §4.3) the reflected sound power P_R and the transmitted sound power P_T. These are simply given in terms of upstream and downstream sound powers taking appropriate account for the change of incidence direction as follows (recall that the acoustic wave is incident from upstream if $\sin(\varphi - \alpha_0) < M\sin\alpha_0$):

$$\begin{aligned} P_R &= \begin{cases} P_U, & \text{if } \sin(\varphi-\alpha_0) < M\sin\alpha_0, \\ P_D, & \text{if } \sin(\varphi-\alpha_0) > M\sin\alpha_0, \end{cases} \\ P_T &= \begin{cases} P_D, & \text{if } \sin(\varphi-\alpha_0) < M\sin\alpha_0, \\ P_U, & \text{if } \sin(\varphi-\alpha_0) > M\sin\alpha_0. \end{cases} \end{aligned} \tag{25}$$

In Fig. 10 we see the contribution of each individual term as a percentage of the overall outgoing power – the reflected and transmitted sound power, hydrodynamic power, and conversion between acoustic energy and kinetic energy in the vortical field. The results in the graph correspond to a stagger angle of $\alpha_0 = \pi/6$, a blade separation of $c = 1$, a Mach number of $M = 0.3$ and a reduced frequency with $\Omega M = \pi/4$.

The curves in Fig. 10 are cumulative, so that for instance the value of P_H is given as the difference of the curve marked with diamond shapes and the curve marked with circles. The vertical dashed lines marked with ■ and ▲ respectively correspond to the values of φ which separate downstream ($\varphi - \alpha_0 \in (9^\circ, 171^\circ)$) and upstream ($\varphi - \alpha_0 \in [0^\circ, 9^\circ) \cup (171^\circ, 360^\circ]$) incident regimes. Note that the roles of reflected and transmitted fields are reversed at these vertical lines, such that for $\varphi - \alpha_0 \in (9^\circ, 171^\circ)$ the reflected sound power P_R represents the downstream sound power P_D and for $\varphi - \alpha_0 \in [0^\circ, 9^\circ) \cup (171^\circ, 360^\circ]$ the reflected sound power represents to the upstream sound power P_U, and vice versa for P_T (cf. Eq. (25)). The important point to observe is that the purely acoustic contributions to the outgoing energy are everything below the curve marked

with circles in the graph. It is clear that for a range of angles of incidence the acoustic contribution only accounts for a fraction of the total outgoing power, indeed sometimes less than half of it. This means a significant amount of incoming energy is converted to hydrodynamic power (P_H), and absorbed into the vortex sheets (Π_ω). This example is representative for a wide range of numerical experiments that were performed: the acoustic contributions alone account for the significant majority of outgoing power only in very specific cases and generally the conversion of acoustic energy into vortical kinetic energy plays an important role in balancing the incoming and outgoing energy flux.

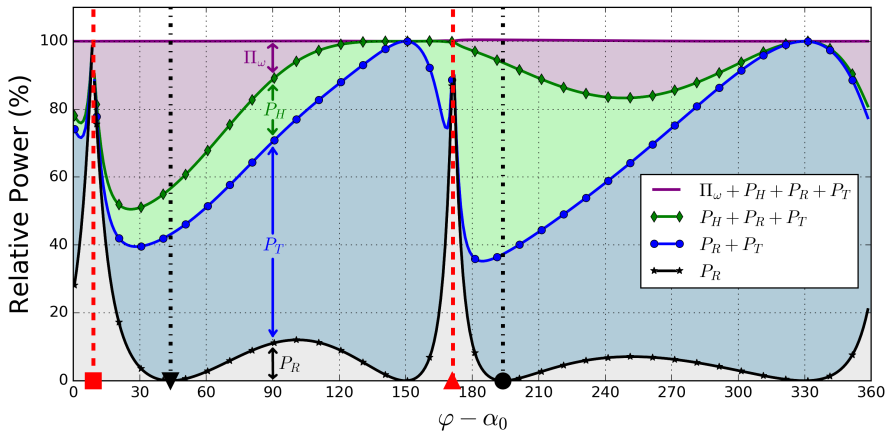

Figure 10: The contributions as percentage of the total incoming power; P_U and P_D are respectively the upstream and downstream acoustic power, P_H is the hydrodynamic power and Π_ω is the sound power absorbed by the wake. The vertical dashed lines (marked with ■ and ▲) separate downstream and upstream incidence and the symbols ▼ and ● correspond to $\tilde{\varphi}_0$ and $\tilde{\varphi}_\pi$ respectively.

4.3. Negative acoustic energy absorption and sound power generation in wave-cascade scattering

An interesting observation was made by Rienstra [29, §4] for a single trailing edge in mean flow: Π_ω can take negative values, which effectively means the blade harvests energy from the flow to increase the total outgoing acoustic and hydrodynamic power (i.e. $P_R + P_T + P_H$) to be greater than the incident power P_I. In some cases this can lead to larger outgoing than incoming acoustic power. We shall see that this effect can also be observed for the cascade of blades, indeed specifically we found the appearance of negative acoustic energy absorption (i.e. acoustic energy emission) by the wake in two scenarios of interest. A particular new contribution in this present work is our detailed parametric study of the size of individual terms $P_R, P_T, P_H, \Pi_\omega$ that constitute the overall outgoing power, which allows us to gain more insight into the consequences of conversion of energy between the acoustic field and the unsteady vortex sheets that takes place at the trailing edge of the cascade blades. One of those insights (which

can be seen in Fig. 14 and which is described in more detail below) is that energy conversion between vortical and acoustic field can, in some cases, lead to over-reflection on the cascade – i.e. the reflected wave can be larger in amplitude than the incoming wave $|R_0| > |I|$.

Acoustic energy emission of the wake near modal cut-on

In Fig. 11 we plot the relative acoustic power $P_A = P_R + P_T$ and the hydrodynamic power P_H as well as their sum (we have rescaled all quantities by P_I) on a decibel scale (i.e. we plot for example $10\log_{10}(P_A/P_I)$). The geometry in this case is taken to be $s = 1, d = 0$, and we choose $\varphi = 4\pi/3$ and $M = 0.75$.

Whenever the black curve (marked with stars) rises above 0 in the graph, we have $P_H + P_A > P_I$, i.e. the acoustic energy absorbed by the wake Π_ω must be negative. Interestingly, we observe this phenomenon at those frequencies just below acoustic modes $\sigma_m^\pm$ become cut-on. In the figure these cut-on values of the reduced frequency Ω are highlighted by the vertical dashed curves – the first one of these corresponds to the horizontal dashed line in the dispersion diagram in Fig. 2. The following trend becomes apparent (as was also observed by Glegg [7, §5.3] for the purely acoustic part of the power): just before a new mode becomes cut-on the hydrodynamic power rises and the acoustic power falls, but sometimes their sum reaches values greater than the incoming power. This is followed by a rapid decay in hydrodynamic power and an increase in acoustic power as the frequency is increased further. Indeed, we may also infer from this figure that for larger frequencies Ω the hydrodynamic effects (both in terms of P_H and Π_ω) play a significant role only close to modal cut-on and that the attenuation of sound is especially pronounced at lower frequencies, which is similar to the observations made by Bechert et al. [23].

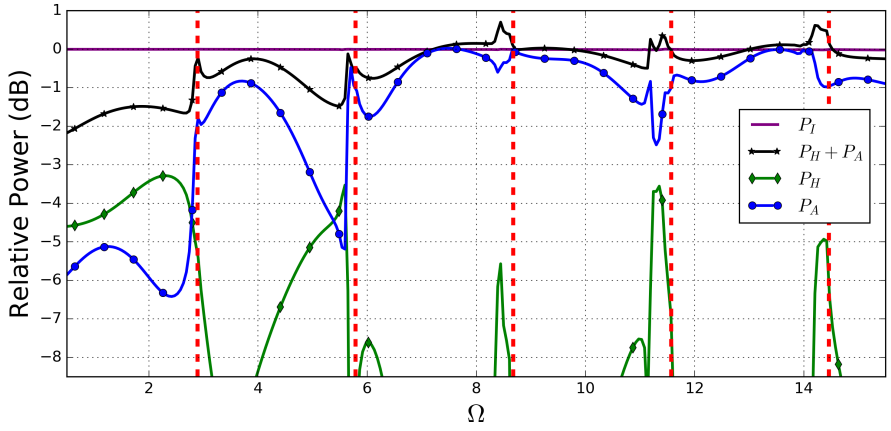

Figure 11: The acoustic and hydrodynamic power for varying incident frequency (dB scale, i.e. we plot for example $10\log_{10}(P_A/P_I)$). The vertical dashed lines highlight the frequencies where new propagating modes become cut-on.

Sound power generation and over-reflection

Finally, we highlight that even for fixed frequencies the acoustic energy absorbed by the wake Π_ω can become negative for specific values of M and φ. The effect is particularly pronounced for downstream incidence and large subsonic Mach numbers, which in some cases results in a reflection amplitude that is larger than the incoming amplitude, i.e. $|R_0| > |I|$. In Figs. 12-14 we plot the relevant quantities from the energy balance for various values of M and φ. The cascade geometry in this case is $\alpha_0 = \pi/6, c = 1$ and the incident frequency is $\Omega M = \pi/4$.

In Fig. 12 we see the energy absorbed by the wake relative to P_I (i.e. Π_ω/P_I) on a linear scale. Note the rescaling by P_I is to ensure that we consider the amount of energy flux relative to the amount of incident sound power provided by the incident acoustic wave. This means we are interested in the 'cascade response' towards excitation from an incident field of fixed amplitude I. Because the problem is linear the energy flux terms will depend on $|I|^2$ and rescaling ensures the results are independent of I. The solid white lines highlight contours of constant $\Pi_\omega = 0$. We observe the absorbed energy can become negative for a range of angles of incidence. As is the case for a single trailing edge (cf. [29, Fig. 3]), the majority of this region of acoustic energy emission occurs when the waves are incident from downstream (i.e. when $\sin(\varphi - \alpha_0) > M \sin \alpha_0$). It is precisely in these regions that amplification of the outgoing acoustic power can occur.

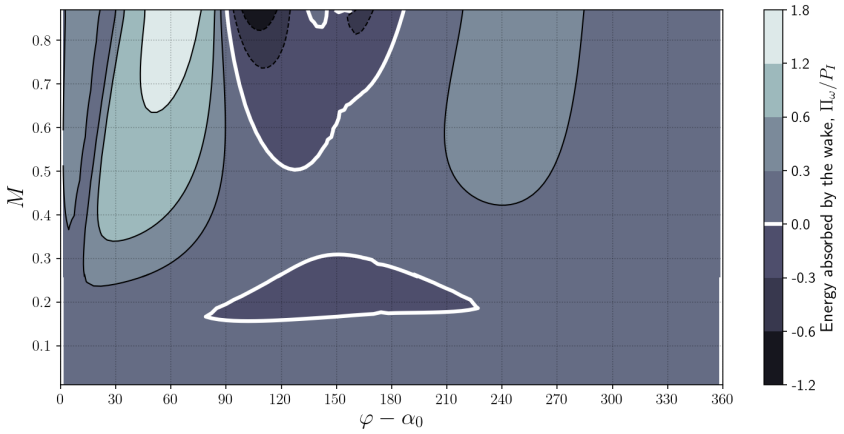

Figure 12: Relative acoustic energy absorption by the wake (linear scale), the solid white line marks $\Pi_\omega = 0$.

Indeed looking at Fig. 13 (which shows the relative outgoing sound power on a decibel scale) we observe that for large Mach numbers, and when $\varphi - \alpha_0 \approx 105°$, this amplification is indeed observed in practice. In fact, we find in Fig. 14 (which shows the relative reflected sound power on a decibel scale) that for a part of this parameter region we even have $P_R > P_I$, i.e. $|R_0| > |I|$, which

means that the incident wave is over-reflected.

We also observe in Fig. 13 that there is significant attenuation of sound over a large range of directions of incidence. This attenuation is due to the conversion of sound into energy in the wake through the shedding of unsteady vorticity at the trailing edge, and the attenuation is found to be greater for larger Mach numbers.

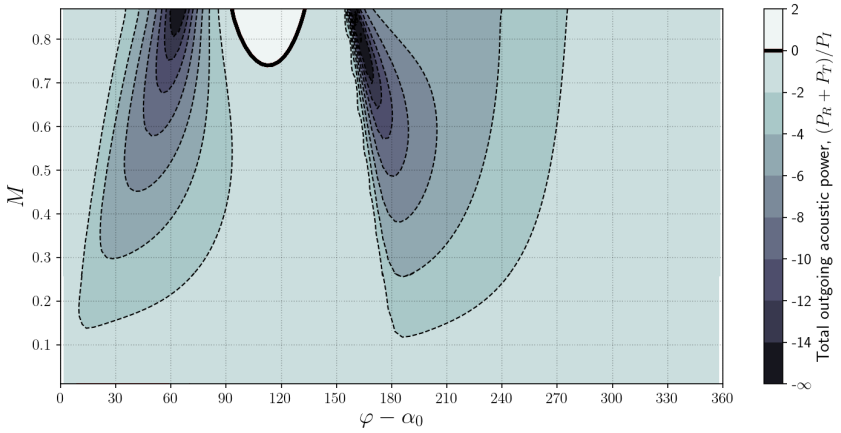

Figure 13: Total outgoing sound power (dB scale), the solid black line marks $P_R + P_T = P_I$.

Finally, we highlight that in Fig. 14 for every fixed value of M the four dark regions contain isolated zeros of P_R at $\varphi = \tilde{\varphi}_0, \pi, \tilde{\varphi}_\pi, 0$ in this order as described in §4.1 (i.e. for any fixed value of M the ratio P_R/P_I takes the value $-\infty$ on the decibel scale at four distinct values of φ).

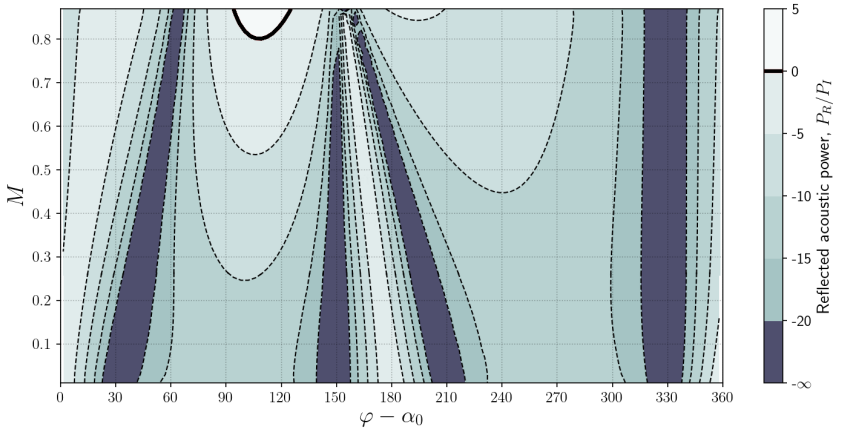

Figure 14: Reflected sound power (dB scale), the solid black line marks $P_R = P_I$.

5. Conclusions

In this work we studied the energy balance for a cascade of flat plates in uniform mean flow. We showed that the outgoing power is composed of acoustic and hydrodynamic power as well as energy flux into the wake, all of which, in general, yield a non-negligible contribution to the outgoing energy flux. Specifically, we provided numerical evidence that there is significant attenuation of sound over a large region of Mach numbers and angles of incidence for incoming sound waves, and that this effect is particularly pronounced at low frequencies. We also found numerical evidence of sound power generation when the waves are incident from downstream and showed the generated power can result in a reflected wave with amplitude greater than the incident one.

Finally, we showed that this energy balance can be used to understand symmetries of the field in the angle of inclination of the wave fronts with respect to the cascade face when there is no mean flow as well as the effect of zero acoustic reflection at certain angles of incidence with mean flow.

Future research will focus on studying the effect loaded blades and non-parallel flow based on the asymptotic solution of the scattering problem on a cascades of blade in non-parallel mean flow provided by Peake & Kerschen [8, 9] which is valid for large frequencies and small nonzero angles of attack. A further direction for future research is the study of the stability of outgoing waves when a small amount of viscosity is introduced to the body of the fluid, in the context of previous work by Benjamin [41] and Cairns [42].

6. Acknowledgements

The authors are honoured to dedicate this paper to the memory of Professor Shôn Ffowcs Williams, who sadly passed away on 12 December 2020 at the age of 85. Shôn was undoubtedly one of the founding fathers of aeroacoustics, whose seminal contributions will surely be talked about as long as people work in our subject. One of us (NP) acknowledges with much affection Shôn's support, advice and friendship spanning more than 30 years.

The authors would also like to thank Lorna J. Ayton and Matthew J. Priddin from the University of Cambridge for several helpful conversations. We gratefully acknowledge support from the UK Engineering and Physical Sciences Research Council (EPSRC) grant EP/L016516/1 for the University of Cambridge Centre for Doctoral Training, the Cambridge Centre for Analysis.

References

[1] G. Maierhofer, N. Peake, Wave scattering by an infinite cascade of non-overlapping blades, J. Sound Vib. 481 (2020) 115418.

[2] J. E. Ffowcs Williams, D. L. Hawkings, Sound generation by turbulence and surfaces in arbitrary motion, Proc. R. Soc. A 264 (1151) (1969) 321–342.

[3] D. G. Crighton, The Kutta Condition in Unsteady Flow, Annu. Rev. Fluid Mech. 17 (1) (1985) 411–445.

[4] W. Koch, On the transmission of sound waves through a blade row, J. Sound Vib. 18 (1) (1971) 111–128.

[5] N. Peake, The interaction between a high-frequency gust and a blade row, J. Fluid Mech. 241 (1992) 261–289.

[6] N. Peake, The scattering of vorticity waves by an infinite cascade of flat plates in subsonic flow, Wave Motion 18 (3) (1993) 255–271.

[7] S. A. Glegg, The response of a swept blade row to a three-dimensional gust, J. Sound Vib. 227 (1) (1999) 29–64.

[8] N. Peake, E. J. Kerschen, Influence of mean loading on noise generated by the interaction of gusts with a flat-plate cascade: upstream radiation, J. Fluid Mech. 347 (1997) 315–346.

[9] N. Peake, E. J. Kerschen, Influence of mean loading on noise generated by the interaction of gusts with a cascade: downstream radiation, J. Fluid Mech. 515 (2004) 99–133.

[10] I. Evers, N. Peake, On sound generation by the interaction between turbulence and a cascade of airfoils with non-uniform mean flow, J. Fluid Mech. 463 (2002) 25–52.

[11] P. J. Baddoo, L. J. Ayton, An analytic solution for gust-cascade interaction noise including effects of realistic aerofoil geometry, J. Fluid Mech. 886 (2020) A1.

[12] P. J. Baddoo, L. J. Ayton, Acoustic scattering by cascades with complex boundary conditions: compliance, porosity and impedance, J. Fluid Mech. 898 (2020) A16.

[13] R. H. Cantrell, R. W. Hart, Interaction between Sound and Flow in Acoustic Cavities: Mass, Momentum, and Energy Considerations, J. Acoust. Soc. Am. 36 (4) (1964) 697–706.

[14] W. Möhring, Zum Energiesatz bei Schallausbreitung in stationär strömenden Medien [On the law of energy conservation of acoustic waves in stationary flowing media], Z. Angew. Math. Mech. 50 (1970) 196–198.

[15] W. Möhring, On energy, group velocity and small damping of sound waves in ducts with shear flow, J. Sound Vib. 29 (1) (1973) 93–101.

[16] C. Morfey, Acoustic energy in non-uniform flows, J. Sound Vib. 14 (2) (1971) 159–170.

[17] M. E. Goldstein, Aeroacoustics, McGraw-Hill, New York, 1976.

[18] M. K. Myers, An exact energy corollary for homentropic flow, J. Sound Vib. 109 (2) (1986) 277–284.

[19] M. K. Myers, Transport of energy by disturbances in arbitrary steady flows, J. Fluid Mech. 226 (1991) 383–400.

[20] M. J. Lighthill, On sound generated aerodynamically I. General theory, Proc. R. Soc. A 211 (1107) (1952) 564–587.

[21] J. E. Ffowcs Williams, L. H. Hall, Aerodynamic sound generation by turbulent flow in the vicinity of a scattering half plane, J. Fluid Mech. 40 (4) (1970) 657–670.

[22] D. G. Crighton, Radiation from vortex filament motion near a half plane, J. Fluid Mech. 51 (2) (1972) 357–362.

[23] D. Bechert, U. Michel, E. Pfizenmaier, Experiments on the transmission of sound through jets, 4th AIAA Aeroacoustics Conference, Atlanta GA, October 3-5 (1977).

[24] M. S. Howe, Attenuation of sound in a low Mach Number nozzle flow, J. Fluid Mech. 91 (2) (1979) 209–229.

[25] M. S. Howe, The dissipation of sound at an edge, J. Sound Vib. 70 (3) (1980) 407–411.

[26] M. S. Howe, On the Absorption of Sound by Turbulence and Other Hydrodynamic Flows, IMA J. Appl. Math. 32 (1-3) (1984) 187–209.

[27] M. S. Howe, Acoustics of Fluid-Structure Interactions, Cambridge Monographs on Mechanics, Cambridge University Press, Cambridge, 1998.

[28] S. W. Rienstra, Acoustic radiation from a semi-infinite annular duct in a uniform subsonic mean flow, J. Sound Vib. 94 (2) (1984) 267–288.

[29] S. W. Rienstra, Sound diffraction at a trailing edge, J. Fluid Mech. 108 (1981) 443–460.

[30] M. S. Howe, The dissipation of sound at an edge, J. Sound Vib. 70 (3) (1980) 407–411.

[31] Y. P. Guo, Sound diffraction and dissipation at a sharp trailing edge in a supersonic flow, J. Sound Vib. 145 (2) (1991) 179–193.

[32] S. Arzoumanian, Stability of fluid-loaded structures, Ph.D. thesis, University of Cambridge (2011).

[33] D. G. Crighton, J. Oswell, Fluid loading with mean flow. I. Response of an elastic plate localized excitation, Philos. Trans. R. Soc. A 335 (1639) (1991) 557–592.

[34] R. Porter, Plate arrays as a perfectly-transmitting negative-refraction metamaterial, Wave Motion 100 (2021) 102673.

[35] D. S. Whitehead, Vibration and Sound Generation in a Cascade of Flat Plates in Subsonic Flow, Aeronautical Research Council Reports and Memoranda (3685) (1970).

[36] S. N. Smith, Discrete Frequency Sound Generation in Axial Flow Turbomachines, Aeronautical Research Council Reports and Memoranda (3709) (1972).

[37] G. Maierhofer, Analytical and numerical techniques for wave scattering, Ph.D. thesis, University of Cambridge (2021).

[38] L. Prandtl, Tragflügeltheorie. I. Mitteilung [Theory of airfoils, Part I], Nachr. Ges. Wiss. Göttingen, Math.-Phys. Kl. (1918) 451–477.

[39] P. G. Saffman, Vortex Dynamics, Cambridge Monographs on Mechanics, Cambridge University Press, Cambridge, 1993.

[40] D. S. Jones, Aerodynamic Sound Due to a Source Near a Half-Plane, IMA J. Appl. Math. 9 (1) (1972) 114–122.

[41] T. B. Benjamin, The threefold classification of unstable disturbances in flexible surfaces bounding inviscid flows, J. Fluid Mech. 16 (3) (1963) 436–450.

[42] R. A. Cairns, The role of negative energy waves in some instabilities of parallel flows, J. Fluid Mech. 92 (1) (1979) 1–14.